Introduction to time-resolved spectroscopy

With applications in biophysics and physical chemistry

Contents

1. Fast processes and ways to see them

In physics, chemistry and biology, a lot of effort and research is directed to understand the dynamics of various processes. To put it simply, people like to watch system parameters changing over time. Depending on the size of the object being watched, the time scales on which the changes take place may vary from very slow to extremely fast (from human perspective). We can try to list several of such processes and arrange them in a table (see also Fig. 1):

Process	Typical duration	Examples
Evolution of species	0.4 million years ($1.2 \cdot 10^{13}$ s)	*homo rhodesiensis* to *homo sapiens*
Population formation	100 years ($3 \cdot 10^{9}$ s)	Takes forest to grow
Animal lifetime span	65.4 years ($2 \cdot 10^{9}$ s) 40 days ($3 \cdot 10^{6}$ s)	A statistical Lithuanian[1] housefly
Animal movement	1 s 0.01 s	Hand gesture Hummingbird wing flap
Biochemical reaction	20 s 0.01 s 10^{-3} s 10^{-5} s	Protein synthesis Complex enzymatic reaction (e.g., ATP synthase produces ATP molecule from ADP and phosphate) Action potential change in a neuron Signalling state formation in a bacterial photoreceptor PYP (photoactive yellow protein) Carotenoid triplet state lifetime in a photosynthetic antenna complex
Elementary biophysical processes	10^{-10} s 10^{-12} s 10^{-13} s	Full charge separation in a photosynthetic reaction centre Excitation energy transfer from photosynthetic antenna to the reaction centre. Retinal isomerization in bacteriorhodopsin and sensory rhodopsin (vision).

[1] 2005 data, life expectancy for Lithuanian males

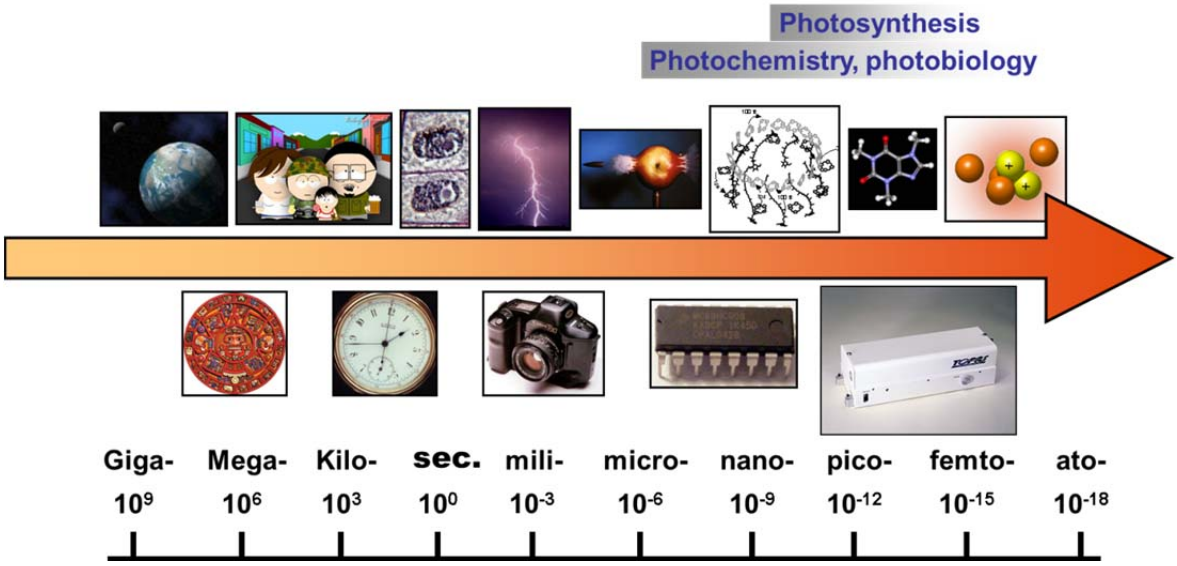

Fig. 1. Different natural processes, their timescales and instruments for following them.

It is obvious that biological processes cover the timescales spread over at least 26 orders of magnitude. This dynamic range is enormous – no single instrument can cover it. Therefore, different tools are required in order to follow different processes. The slowest tool we have is probably a calendar; more scientifically oriented of us will prefer radioactive dating methods. They follow the processes stretched over centuries and millennia. Further down, on the time scales of human lives, one would probably use a newspaper or a chronicle to describe them. Even faster events are recorded using fast film cameras or photographic cameras with short exposure times (useful, for example, for sport events or monitoring how a lion is chasing a gazelle, timescales down to 0.001 s). Electronic devices provide access to the realm of microseconds, nanoseconds, down to hundreds of picoseconds. Even faster processes, the durations of which are tens of picoseconds and less, require the fastest tool available in nature – light itself. Light (and other electromagnetic waves) travel in vacuum at the constant speed of roughly $3 \cdot 10^8$ m/s. To visualize it better, let's look at another table with familiar distances and the time intervals it takes light to travel them:

1 s	300 000 km	Mileage of an average car from manufacturing to recycling
1 ms	300 km	Similar to distance from London to Paris (344 km)
1 μs	300 m	Roughly perimeter of a football field
1 ns	30 cm	Large male foot
1 ps	0.3 mm	Thickness of the beer can walls
1 fs	0.3 μm	Thickness of the rainbow-colored oil film on a puddle

Comparison of the two tables immediately shows that some biological processes happen so fast that even the fastest thing known (light) manages to cover a distance of some microns during the entire event. Let us designate (somewhat arbitrarily) all the processes happening faster than within 1 μs *ultrafast processes.* The area of science that explores ultrafast processes in atoms, molecules, crystals and glasses using light-based spectral techniques is called time-resolved (or ultrafast) spectroscopy.

Ultrafast phenomena are tough to handle even using light, fast as it may be. Therefore, in order to investigate them, light needs to be controlled in an especially precise manner. The light sources providing unprecedented control of light parameters are lasers. They have been invented in 1960, and have since reached perfection allowing the scientist to control fully such light properties as

- Intensity,
- Color (wavelength)
- Direction
- Duration of pulse (flash)
- Polarization
- Phase

It is this unprecedented degree of control over light, laser spectroscopy is a gold mine in investigating ultrafast phenomena. Further we will discuss the general principles of the lasers used for time-resolved spectroscopy; after that, we will describe several most popular time-resolved spectroscopic techniques used in investigating ultrafast phenomena in biology and chemical physics.

2. Light sources for ultrafast spectroscopy

2.1. Generation of ultrashort pulses: principles and methods

In order to follow ultrafast events, an experiment needs *time resolution.* In other words, the equipment used must involve a component changing faster (or, at least, as fast) than the process under investigation. For example, in order to follow the motion of hummingbird wing during the flight (Fig. 2), the camera must allow exposure times so short, that the motion of the wing during the exposure period is negligible: if hummingbird flutters its wing in 0.01 s, the exposure time of the camera has to be as short as 1/1000 s. In conventional cameras, the exposure time is controlled by a shutter – a mechanical device. Obviously, it cannot open and close in picoseconds (a millisecond is already a challenge).

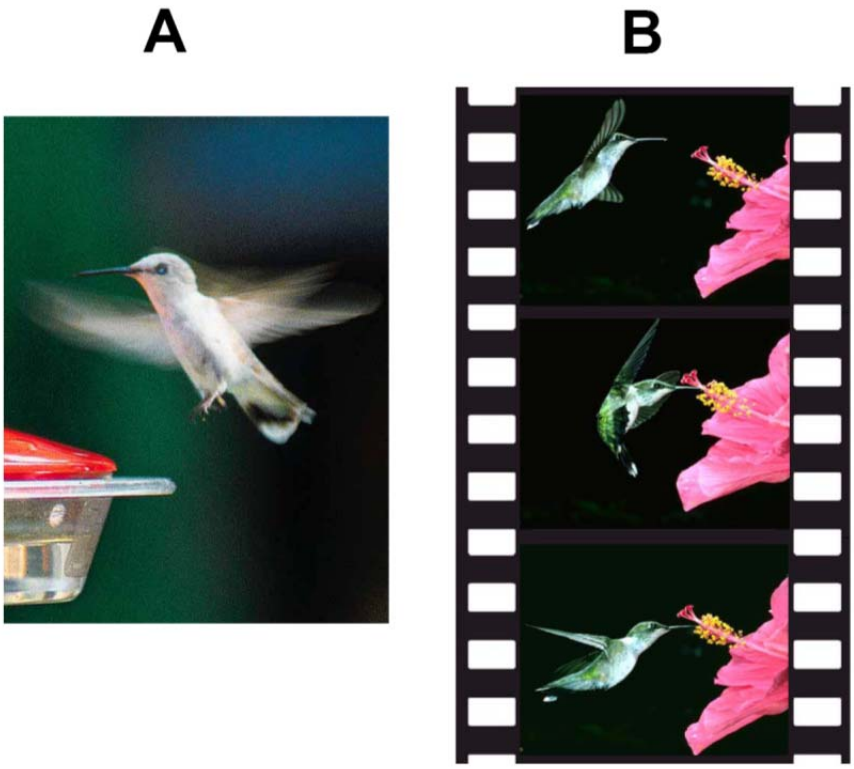

Fig. 2. A: Picture of a hummingbird using standard 1/60 s exposure. A flap of the wing occurs several times during the exposure time and the wing is blurred in the picture. B: Hummingbird flight recorded using fast (1/1000s) exposure. Every frame shows a clear view of hummingbird wing.

As we already know, the role of camera shutter in ultrafast spectroscopy is played by a fast-changing light parameter, namely its intensity given by the square of the amplitude of the electric field. In other words, time resolution in ultrafast spectroscopy comes from short laser flashes called pulses. In the following, we will concentrate on the equipment issues of ultrafast spectroscopy: how to make a laser to produce short light flashes, and how to make the particular kind of light required for time-resolved experiments.

The principle of laser is described in any self-respecting physics textbook [1] and we will assume that the readers are familiar with them. Fo those willing to wade deeper into the subject, excellent textbooks with extensive treatments of ultrafast laser technology are also readily available [2]. The introductory material here should be seen as a 'quick and dirty way' to get to grips quickly with the necessary issues, rather than a properly detailed description.

So, how do we make a laser to produce light pulses instead of a continuous light (laser people call the latter 'continuous-wave' or cw operation of laser)? Depending on the duration and energy of the pulses we want to produce, two engineering solutions are available to make a laser pulse:

- Q-switch or a variable attenuator inside the laser cavity (usually resulting in high-energy pulses with the duration of several nanoseconds)
- Mode-locking of the light modes inside the laser cavity (for obtaining pico- and femtosecond pulses).

Let us discuss them both in detail.

2.1.1. Q-switched lasers produce high energy nanosecond pulses

Q-switch or a variable attenuator in the laser cavity is a technique for obtaining powerful laser pulses. As name suggests, the idea is introducing *variable* losses in the laser cavity. The changes in losses result in the different quality factor (Q-factor) of the laser cavity, hence the name Q-switch. Any oscillator, including a laser is an amplifier with positive feedback (meaning that part of the output signal is returned to the input of the amp. In the laser, the pumped active medium acts as an amplifier for light, whilst the cavity mirrors provide the positive feedback, returning part of the produced light into the active medium. When cavity losses are on, the light that has left the active medium cannot come back and the positive feedback required for lasing does not occur. Therefore, even hard pumping of active medium does not result in lasing. This allows creating very strong population inversion, i.e. promoting almost all the atoms of the active medium into their metastable

excited states. When the losses are switched off, the Q-factor of the cavity suddenly increases (the feedback appears), and the laser starts lasing. Because the active medium has stored a large amount of energy, the gain of the amplifier is very high and the intensity of laser radiation grows extremely fast. It also disappears very fast, and for the same reason: high intensity radiation produced quickly 'eats away' all the population inversion. This way, the so-called giant pulses are produced. Typically, Q-switched lasers produced by different companies us Nd:YAG or Nd:YLF as their active media; they produce pulses with the duration around 10 ns, the energies of which can be in excess of 1 J.

Technically, Q-switching is usually performed using one of the three major methods. The variable loss component of the cavity can be

- Saturable absorber
- Electro-optic modulator
- Acousto-optic modulator.

A saturable absorber is an optical medium that absorbs laser radiation. When most of its atoms are in their ground state, the medium absorbs the laser light and the losses in the cavity are high. However, when most of the absorber atoms become excited, the medium becomes transparent and cavity losses suddenly decrease. Obviously, such modulator is *passive*, i.e. no external control is necessary (Fig. 5A).

One of the most common active Q-switches is an electrooptic Pockels cell. It is a crystal where high voltage (usually several kV) induces birefringence and makes it act as a half-lambda phase plate. In other words, the phase difference between an ordinary and extraordinary waves passing the crystal becomes equal to π. When linearly polarized light impinges on such crystal at with its polarization axis at 45° to the ordinary axis, its polarization plane gets rotated by 90°. Along with a crystal, a polarizer is inserted into the cavity. When the high voltage is off, the polarization of light generated in the cavity is such that the polarizer blocks it – the losses of the cavity are high and no lasing can occur. When the gain medium accumulates enough population inversion, half-lambda voltage is switched on, the light polarization is rotated and the beam can pass through the polarizer

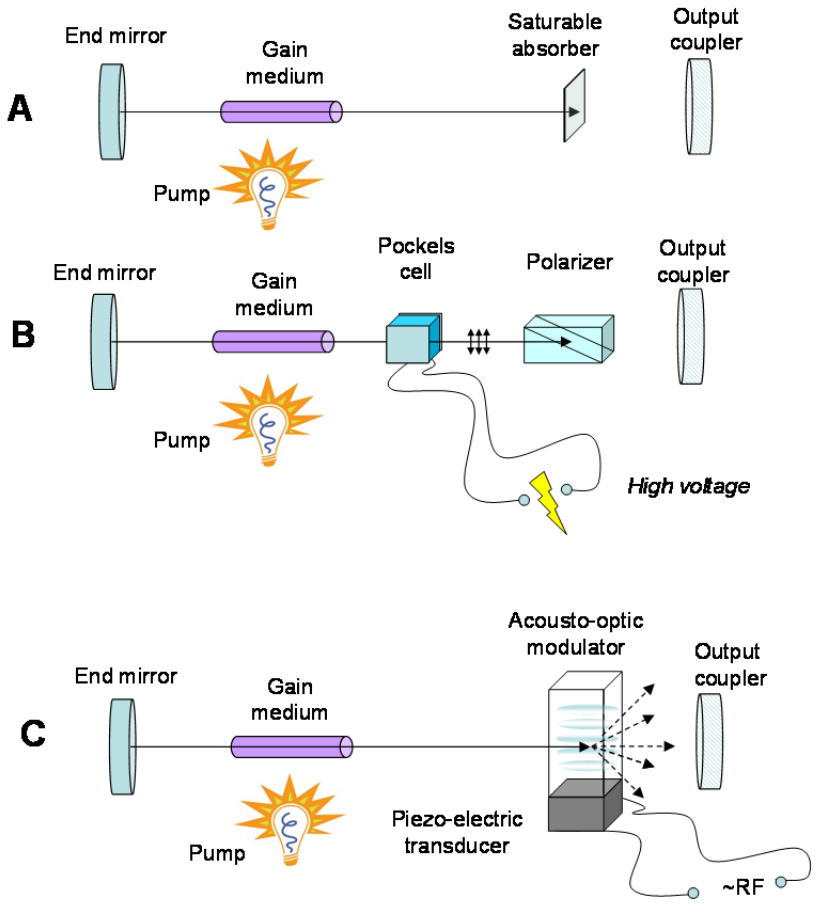

Fig. 3. Laser cavities with different Q-switches. A – saturable absorber, B – electro-optic modulator (Pockels cell), C –acousto-optic modulator. RF denotes radio frequency electrical field used to excite piezoelectric transducer and generate a standing acoustic wave in the crystal.

without losses. This results in a giant light pulse, which sweeps down the accumulated population inversion. Pockels cells (Fig. 3B) are used in lasers with different repetition rates – from several Hz to 1 MHz. They are called active because they are actively controlled by an external high voltage source.

Another type of an active Q-switch is an acousto-optic modulator. It consists of a piece of transparent material (e.g. glass or quartz), where a standing acoustic (ultrasound) wave is produced using piezoelectric effect. To achieve this, the transparent material is attached to a piezoelectric transducer – a slab of material with piezoelectric properties (e.g. $BaTiO_3$). Standing acoustic wave produces periodic modulation of refractive index in the material – a phase grating. Laser radiation is diffracted by this grating, changes its direction of propagation and leaves the cavity. When RF field is switched off, the grating disappears and all the light is transmitted by the transparent material. The lasing starts and giant laser pulse is produced (Fig. 3C). Typically, acoust-optic Q-switches produce pulses of hundreds of nanoseconds.

Q-switched lasers are widespread, and wider description is available in the literature [3]. They are widely used for the investigation of nano-, microsecond and longer processes, flash-photolysis spectroscopy. They are also useful as pump (energy) sources for other (e.g. femtosecond) lasers.

2.1.2. Ultrashort pulses and longitudinal modes of the cavity

The most interesting (and most difficult to access) processes take place in this very pico- and femtosecond time range. To get light pulses with the durations in this range, one needs to use modelocked lasers. Here we will briefly introduce the principles of modelocking and discuss its importance for the production of ultrashort light pulses.

We already said that a laser is an amplifier of electromagnetic waves with positive feedback. (The well-known example of this is a microphone-amplifier-loudspeaker system, where bringing the microphone too close to a loudspeaker produces a nerve-wrecking whistle. The oscillation starts, when a bit of noise is picked up by microphone, amplified, emitted by a loudspeaker, picked up by the microphone again, amplified again, and wheeeee!). So, a laser does a similar trick with light. It consists of an active medium, were photons traveling in the gain medium produce their twin brothers

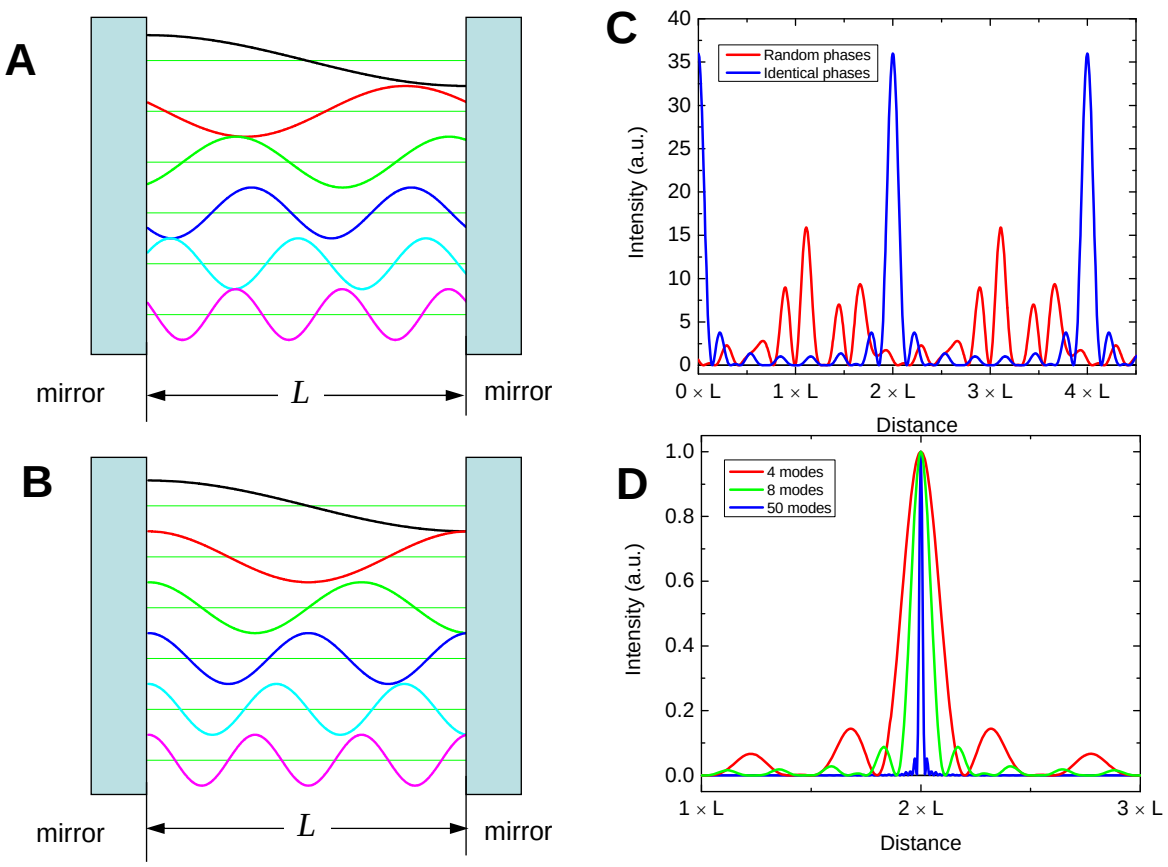

Fig. 4. Longitudinal modes in laser cavity: A: modes with randomphases (at the start of the cavity some curves are rising, others are falling); B – modes with identical phases (all curves are at their maxima and start to descend at the beginning of the cavity). C – field intensity resulting from a superposition of 6 modes with random phases (red line) and identical phases (blue line). D – the pulses resulting from the superposition of 4 (red), 8 (green) and 50 modes.

via stimulated emission. The light is contained within the laser cavity by (at least) two mirrors, one of which is semitransparent. The leaked out light is the useful laser output, whereas the light that stays in the cavity gives the positive feedback for the amplifier. So, the light travels back and forth in the cavity and is amplified, as shown in fig. 4. Note that although the laser cavity in fig. 4 consists of only two mirrors, more complicated configurations are often employed. However, for the explanation of principles, this simple cavity is sufficient. Such cavity is optically indistinguishable from Fabry-Perot etalon, i.e. it acts as a frequency filter: the only wavelengths that constructively interfere with themselves upon reflection from the mirrors and survive in the cavity are the ones that satisfy the condition:

$$n\frac{\lambda}{2} = L,\ n = 1, 2, 3... \qquad (1).$$

In other words, for a wave to survive in the cavity, the integer number of wavelengths has to fit in the cavity length. The waves that satisfy this condition are called *longitudinal modes* of the cavity.

Naturally, the wavelength of light that laser produces also depends on the gain profile of the active medium (i.e. the stimulated emission spectrum). Because the mode frequencies are different, the generation of different modes in the laser cavity starts independently from one another[2], and the mode phases generally are random (fig. 4A). Adding several such fields together and taking the square of the sum, we obtain the intensity of the electric field (light). With random phases, the intensity will be some random periodic function (red line in fig. 4C) with the period that is equal to the double length of the cavity (round trip distance). On the other hand, if we add the modes with identical phases (as in fig. 4B) and take the square of this sum, the resulting intensity will be *a train of pulses*, where the distances between adjacent pulses – again – are equal to the double cavity length. The physical meaning of such periodicity is clear: this is the distance light needs to cover while travelling around the cavity. After covering this distance, light comes back to the output coupler mirror, through which part of the radiation is emitted to the outer world. Therefore, the distance between the pulses in the train is twice the cavity length, and the repetition frequency of the pulses (called laser repetition rate) can be found by dividing the speed of light by this distance.

The more modes we add, the shorter laser pulses will become, because the extent of space (or time) where *all* the modes are at their maxima will be shorter. This dependence is visualized in fig. 4D, where the square of the electric field amplitude, resulting from the superposition of 4, 8 and 50 modes with identical phases, is compared. In other words, the more different colours (frequencies) we add, the shorter pulse will become. This can be demonstrated mathematically. For that, let us describe the electric field of light pulse as an oscillating function (imaginary exponent) with a Gaussian envelope, i.e. a product of a Gaussian envelope and an imaginary exponent:

$$E(t) = E_0 e^{-\frac{t^2}{2\tau^2}} e^{-i\omega_0 t} \qquad (2)$$

Such pulse shape, graphically depicted in fig. 5, is widely used: even if the pulses of many ultrafast lasers are not exactly described by the eq. (2), the approximation is quite good for many purposes.

[2] The mode with every frequency „sees“ only those atoms of the active medium, the stimulated em ission frequencies of which match the frequency of the mode.

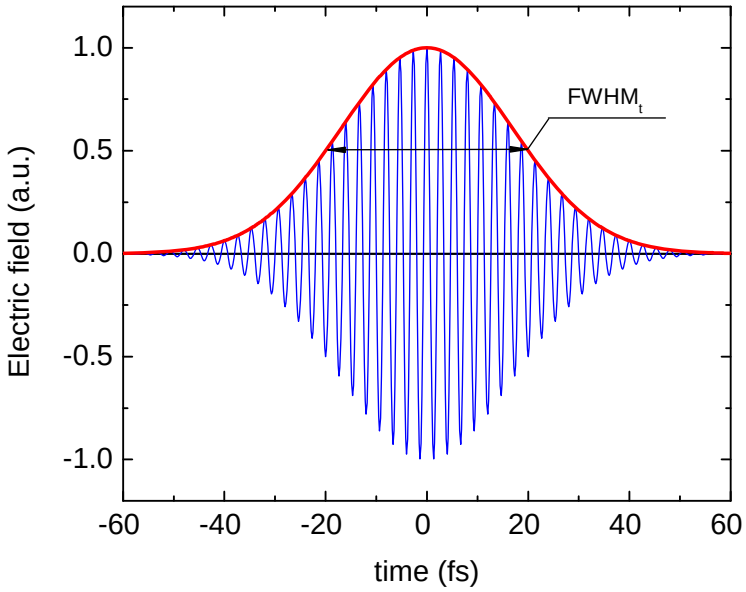

Fig. 5. Electric field (blue line) and amplitude envelope (red line) of a Gaussian pulse. Pulse duration (full width at half-maximum, FWHM, of the amplitude is indicated by the arrow.

Parameter ω_0 is called the central (carrier) frequency of the pulse, and τ is the pulse duration. Instead of τ, the temporal length of the pulse at half the maximum amplitude, full width at half maximum, $FWHM_t$, is often used. Equating the Gaussian envelope in eq. (2) to 0.5, we can easily find the relationship between τ and $FWHM_t$:

$$FWHM = \sqrt{8\ln 2}\,\tau \tag{3}.$$

To find the spectrum of the pulse described by eq. (2), which we can measure by, for example spreading the light of the pulse on a CCD sensor of a camera by a diffraction grating, we take a Fourier transform:

$$E(\omega) = \frac{1}{\sqrt{2\pi}} \int_{-\infty}^{+\infty} E(t) e^{-i\omega t} dt = \frac{1}{\sqrt{2\pi}} \int_{-\infty}^{+\infty} E_0 e^{-\frac{t^2}{2\tau^2}} e^{-i\omega t} dt \tag{4}.$$

This Fourier integral is easily calculated: you just have to supplement the exponent to a full square, i.e. convert it into an integral of the type $\int_{-\infty}^{+\infty} e^{\xi^2} d\xi$, the value of which is known from mathematical physics and is equal to $\sqrt{\pi}$. After collecting all the prefactors, we obtain the spectrum of the pulse described by eq. (2).

$$E(\omega) = E_0 \tau e^{-\frac{\tau^2(\omega-\omega_0)^2}{2}} = E_0 \tau e^{-\frac{(\omega-\omega_0)^2}{2\sigma^2}} \tag{5}.$$

Here we have denoted $\sigma^2 = \frac{1}{\tau^2}$. As we can see, the spectrum of a Gaussian pulse is also a Gaussian function, and its *spectral width* is inversely proportional to the temporal duration, i.e.

$$\tau \cdot \sigma = 1 \tag{6}$$

The constant on the right-hand side of eq. (6), which is equal to one, is called *time-bandwidth product*. Its minimum value is equal to one, in which case we have a "nice" and symmetric Gaussian electromagnetic pulse, which is known as *transform-limited* pulse because its bandwidth is dictated by Fourier transform. If the frequency components are slightly "out of step" in time, this number will be greater than unity. Eq. (6) also shows that the shorter the light pulse, the broader its frequency spectrum (the more different frequencies are present); the same is illustrated by fig. 4D. Equations (2)-(6) are written down for the electric field strength *E*, expressed in terms of angular frequency ω. This form is more convenient mathematically, however, in the lab we deal with the field intensity, which is the square of the electric field, not the field itself. The frequencies are also usually conventional, rather than angular. When these real-life parameters are plugged into the equations, and the square of the electric field is taken, additional prefactors emerge and for a Gaussian pulse, the product between temporal and spectral widths becomes as follows:

$$FWHM_\nu \cdot FWHM_t \approx 0.441 \tag{7}.$$

In this product, the value of frequency bandwidth is expressed in Hz; it is measured as full-width at half maximum of intensity; similarly, the temporal duration is full-width at half intensity maximum expressed in seconds.

2.1.3. Modelocking

In the previous section we demonstrated that in order to get short light pulses, laser must

a) Generate light in as wide frequency range as possible and
b) The modes with different frequencies must have identical phases

Therefore, the first requirement for an ultrashort (1 ps and shorter) pulsed laser is a broad gain spectrum. This explains why gas lasers are not especially attractive for short pulse generation: emission lines of gases are very narrow, which makes it impossible to amplify wide range of frequencies. Therefore, historically first 'real' ultrafast lasers were dye lasers, where the gain profile covers the entire fluorescence spectrum of a dye molecule (which can be up to 50 nm wide in the visible range). Dyes are also not especially attractive as lasing media: organic molecules tend to

degrade when they are excited and de-excited multiple times, therefore, the dye solutions must be circulated for refreshment, employing large and noisy pumps. When hoses crack, dyes spray over the entire lab, making almighty mess. Some dye molecules have even been found to be carcinogenic. Additionally, wavelength tuning with a single dye is only possible across a relatively narrow spectral range. For different range of wavelengths, dyes must be replaced – a long and messy process. For these reasons, laser engineers found a way to replace dyes with solid state media: almost all biophysical and physicochemical research uses ultrafast lasers based on titanium-doped sapphire (Ti:Sapphire, Ti:Al_2O_3) lasers allowing the generation of light in the spectral range from 690 to 1050 nm. The maximum gain is around 800 nm, which is the wavelength corresponding to the carrier frequency of Ti:Sapphire pulses. In the recent years, solid-state lasers employing other active media, such as Yb:KGW crystals have gained in popularity, but Ti:Sapphire remains a main workhorse of ultrafast science.

So, how do we make the laser to generate all the modes in step (with equal phases)? The general idea is that, similarly to a Q-switched laser, laser cavity must be supplemented by a component that damps the lasing action (increases cavity losses), when the laser operates in continuous wave (cw, random mode phases) regime. On the other hand, this component should encourage lasing when the phases of different modes (accidentally) fall in step. There are several solutions for this, but we will only discuss one, called *Kerr lens modelocking*, because this is one of the simplest and most widely used modelocking mechanism in Ti:Sapphire laser systems.

Kerr effect in optics is the dependence of refractive index of a medium on the intensity of the light propagating therein. In such medium, the refractive index can be described in the following way:

$$n = n_0 + n_1 I \qquad (8),$$

where n_0 is the conventional (linear) refractive index, observed at low light intensities. A laser beam intensity distribution in the plane perpendicular to the beam propagation direction is usually similar to Gaussian, i.e. the intensity is low at the sides and high at the center. When such beam propagates in the medium with nonlinear refractive index, the refractive index change is highest in the center and lowers at the edges. Thus, the medium obtains refractive index profile similar to that of a lens and the beam starts to focus (fig. 6A). The tighter the focusing is, the higher is the intensity of the beam, and the stronger lensing effect can be achieved. Therefore, when the beam starts to self-focus, it will keep contracting in size until other phenomena kick in to limit the focus (e.g. diffraction, or

breakdown of the medium). We note that such self-focusing is only possible at high light intensities (because the refractive index change is proportional to the intensity). Now, given the same amount of pump light, the intensity will always be higher in the pulsed regime, where all the energy is concentrated in the peak of the pulse, rather than spread over time. This, in turn, means that self-focusing will be a lot stronger, when the laser is modelocked: all modes are in phase and strong pulse is generated instead of continuous wave operation. Let us now insert an aperture in the cavity (an opaque plate with a hole in the center) that will only allow the focused beam to pass. Then the modelocked light will be able to freely travel in the cavity and be amplified. If the laser is inclined to misbehave and lase with randomly phased modes, such lasing will be discriminated against by the aperture (the beam does not get focused and a large portion of light is stopped by the aperture – losses increase). This way, a "natural selection" of lasing is established: only modelocked light is amplified, and all other types of generation are discriminated against. In fact, when the laser becomes modelocked, it is hard to kick out of this operation regime: the pulsed operation consumes the entire population inversion and CW operation gets no chance to start. Loosely speaking, the laser 'rather waits' for the next pulse than starts lasing in CW – there is simply no juice left after the previous pulse.

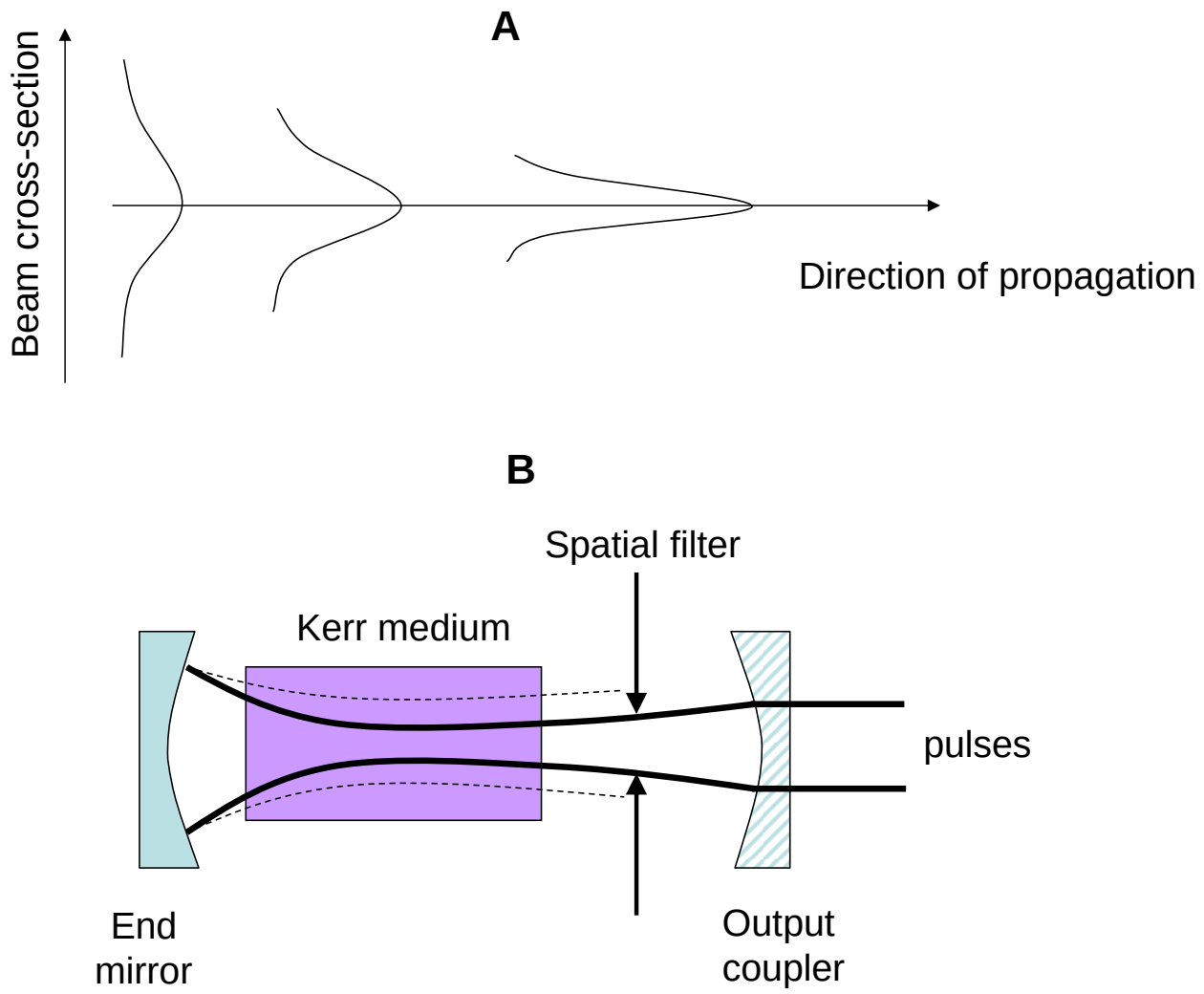

Fig. 6. A: focusing of light due to Kerr effect: when light propagates in nonlinear medium, refractive index change is highest in the center of the beam (where light intensity is high), and lower in the sides (intensity is low). The resulting refractive index profile resembles a lens and focuses the beam. The focused beam results in higher refractive index change, etc. B: modelocking in the laser cavity using Kerr lens. When laser operates in pulsed mode (modes are in phase), the peak intensity in the pulse is higher and the resulting Kerr lens focuses the beam, allowing it to pass the spatial filter: lasing is efficient (thick black line depicts the beam). In CW mode, (thin dashed line), electric field intensity is insufficient for self-focusing to occur and lasing does not start because of the losses on the spatial filter.

Ti:Sapphire laser operating in the described fashion is called an *oscillator*. It will generate a train of pulses, the duration of which can be down to a few tens of femtoseconds (with special care one can get down below 10 fs). The repetition frequency of the pulses matches cavity round trip time, usually around 80 MHz, or 12.5 ns between consecutive pulses. The energies of pulses are in the range of 1-6 nJ.

2.1.4. Pulse amplification

Even though the pulses coming from the oscillator are well suited for some time-resolved spectroscopic experiments, a single Ti:Sapphire oscillator without any amplifiers has several drawbacks:

- Very high repetition rate. The light induced processes in biological systems sometimes take milliseconds, or longer to complete (for example, a triplet state of chlorophyll lives for about 3 ms). If the time intervals between the pulses are shorter than the duration of the investigated processes, every pulse coming to the sample encounters the 'footprints' of previous pulses still present. That renders the experiment incorrect. One way to solve this problem is moving the sample to investigate a fresh spot each time; however with only 12 ns of time between pulses, it is physically impossible to move the sample far enough for the laser beam to interrogate a fresh spot.
- Narrow tuning range. Even though the Ti:Sapphire oscillator is tunable in the range from 700 to 1000 nm, many research tasks require different spectral range – the samples simply do not absorb in the accessible wavelength range. Tuning the wavelength of light is made possible by nonlinear optical devices called optical parametric amplifiers (OPAs), which will be discussed later. However, to operate properly, these usually require higher energies than available from the oscillators. Additionally, some types of time-resolved spectroscopy measure inherently nonlinear signals (e.g. two-photon absorption, photon echo spectroscopy), only observable at high laser field intensities.

To obtain higher pulse energies, a technique called *chirped pulse amplification* is employed. The laser implementing this technique is called *regenerative amplifier*. The amplification sequence is illustrated in fig. 7.

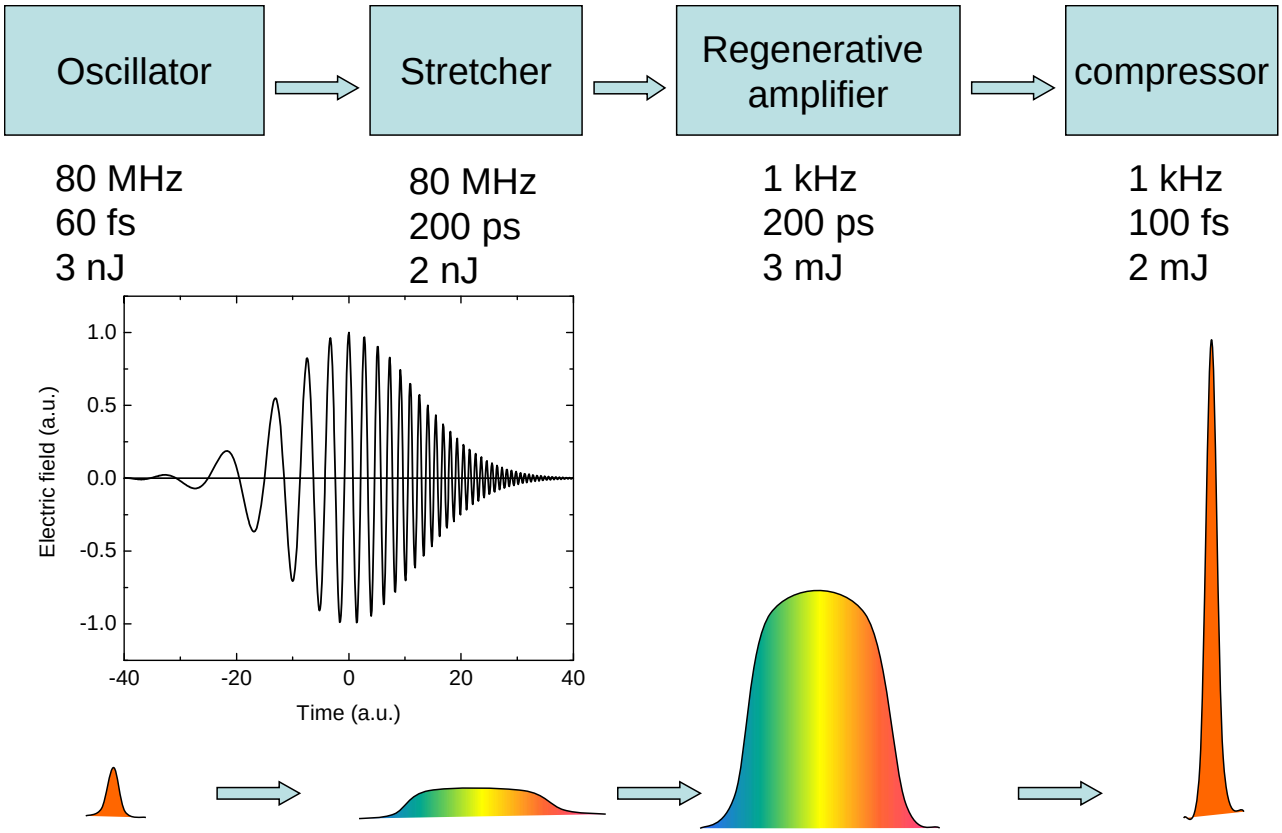

Fig. 7. Operation principle of chirped pulse regenerative amplifier. Weak pulses are stretched in time, one out of ~80000 pulses is injected into the amplifier cavity, amplified and compressed in time again. The inset shows the shape of the electric field in the chirped pulse: lower frequencies (redder photons) arrive first, followed by the higher frequencies (bluer photons).

- Oscillator pulses are stretched in time (i.e. their duration is increased) up to several hundreds of picoseconds.
- One out of roughly 80000 pulses is injected into the cavity with Ti:Sapphire crystal pumped by a Q-switched laser.
- The pulse travels around the cavity several (or more) times, until it is amplified to several mJ of energy.
- Amplified pulse is ejected from the cavity.
- The pulse is compressed (in time) back to several tens or hundreds of femtoseconds.

Stretching before and compressing after the amplification is necessary in order to avoid damage of optical components in the amplifier: if a pulse of 100 fs is amplified and focused in the laser crystal, its peak power becomes so high that the optical components in the amplifier break down.

Pulse stretching and compressing is done using diffraction gratings to spread the pulse spectrum in space and organizing the beam path in such a way that bluer frequency components travel a longer distance (in the stretcher) or shorter distance (in the compressor) than the red ones. An inset in fig. 7 schematically shows the electric field of a chirped pulse, where lower frequencies arrive at the observer earlier than the higher ones. Injection and ejection of pulses into the regenerative amplifier cavity is done using electronically controlled Pockels cells and reflective polarizers (their action is virtually identical to that of an electro-optical Q-switch, see above). More information on chirped pulse amplification is available in literature [4]. After chirped pulse amplification, light parameters are typically as follows: pulse repetition rate – around 1 kHz., duration – around 50 fs, spectral width in the vicinity of 30 nm, pulse energy – 0.5 to 5 mJ.

2.1.5. Nonlinear optical processes: getting the colors necessary for optical spectroscopy

Amplified pulses from Ti:Sapphire lasers can be readily used for time-resolved spectroscopy experiments. One question, however, remains unsolved: what do we do if the system we want to investigate absorbs the light outside the spectral range accessible by Ti:Sapphire lasers (around 800 nm). How do we get light, at, say 670 nm? It is clearly impractical to construct a new laser each time you get a new sample in your lab. Wavelength tuning and getting colors other than 800 nm wavelength is done employing the phenomena of *nonlinear optics.* Nonlinear optics is the entire branch of science investigating optical phenomena occurring when the electric field of light is comparable to that holding the electrons of atoms at the nuclei (roughly 10^{10} V/m). There are entire books on nonlinear optics [5], here we just depict several phenomena employed in getting the right colors for time-resolved spectroscopy.

Dispersion

Sorry for starting the discussion of nonlinear optical phenomena from the phenomenon that is acutally linear. Light dispersion is the phenomenon of linear optics, but it is important for the further discussion, therefore we will say a few words about it. In optics, dispersion is the dependence of refractive index on the frequency (or wavelength) of light. Transparent materials exhibit so-called normal dispersion, i.e. refractive index increases with frequency (or decreases with wavelength). The speed of light in the material is reversely proportional to its refractive index; therefore the blue photons (shorter wavelength) travel more slowly than the red ones. This means that if a transform limited pulse described by eq. (2) passes through a slab of transparent medium (e.g. a piece of glass),

its duration will increase because the photons of different colors spread out and do not reach the observer all at the same time. If the medium exhibits normal dispersion, the red photons will arrive earlier, and the blue ones – later (see the pulse in the inset of fig. 7). Such pulse is called *chirped* and resembles the pulses in the cavity of the regenerative amplifier. Dispersion broadening of the ultrashort pulses is usually an undesirable effect in the time-resolves spectroscopic experiments. It makes the pulses longer and decreases the time resolution of the experiments. To prevent it as much as possible, optical components of femtosecond beam lines (like lenses, waveplates or polarizers) are made as thin as possible. This also prevents transporting femtosecond pulses using optical fibers: in several meters of fiber a femtosecond pulse will stretch to tens of picoseconds, and different frequency components will scatter in time killing any dreams of good time resolution.

Harmonic generation

The easiest way of getting access to different colors than those produced by the laser is harmonic generation. This is truly a nonlinear optical phenomenon. Using harmonic generation from light with frequency ω, we can obtain light with frequencies 2ω, 3ω, etc. The description of harmonic generation (and most of other nonlinear optical phenomena) starts with writing down the expression for nonlinear polarization. From Maxwell's equations of electrodynamics we know that polarization is one source of electric fields (another one is charges). In a general case, material polarization can be written down as power series of electric field strength:

$$P = \varepsilon_0 \left(\chi^{(1)} E + \chi^{(2)} E^2 + \chi^{(3)} E^3 + \ldots \right) \quad (9).$$

In this equation, $\chi^{(i)}$ denotes dielectric susceptibility of the *i*-th order. When electric field is weak, the only significant term in eq. (9) is the first one. This is the linear term describing linear optical phenomena (dispersion, refraction, reflection, etc.) – material polarization is *linearly* propotional to the propagating electric field. Let us assume, that the field is described by a plane electromagnetic wave:

$$E = E_0 e^{-i(\omega_0 t - kz)} \quad (10).$$

Here $k = \frac{2\pi}{\lambda} n = \frac{\omega}{c} n$ is the wave vector (wave number in one-dimensional case). Plugging (10) into (9), and leaving just the first term, we clearly see that no new frequencies will be produced by the polarization. The only thing changing will be the speed of light propagation (in multidimensional

case, the direction may also change). However, if the electric field is strong enough and we cannot neglect the second term in eq. (9), it will become proportional to

$$P^{(2)} \sim e^{i(2\omega_0 t - 2kz)} \quad (11),$$

i.e. material will start producing the light waves with the frequency twice of the incident wave. The same way, we can show that two waves with different frequencies in the medium will result in the waves with the frequencies representing the sum and the difference of the incoming frequencies. The emergence of double frequency is called second harmonic generation, and the general case of such wave interaction (when the incident waves differ in frequencies and come from different directions) – *three-wave mixing* (three, because there are two incoming waves and one generated wave).

From symmetry considerations, one can show that second order nonlinear dielectric susceptibility $\chi^{(2)}$ is zero in all isotropic materials. Therefore, harmonic generation, sum frequency generation and difference frequency generation can practically be realized only in crystals without the center of inversion. In femtosecond spectroscopy β-barium borate (abbreviated BBO) crystal is often used, because it features high optical damage threshold and has large second order dielectric susceptibility, thereby allowing efficient harmonic generation at lower light intensities. In order to generate harmonics efficiently, one needs to fulfil the *phase-matching condition*, which means that both incident wave and the generated wave must travel in the crystal at the same phase velocity (i.e. their respective refraction indices must be equal). This is also realized using crystal anisotropy: the polarization of the generated second harmonic wave is perpendicular to that of the incident wave. Different polarizations 'see' different refractive indices in the crystal. By suitably orienting the crystal, one can achieve the orientation, when both ω and 2ω waves experience identical refractive indices and therefore travel at the same velocities. Besides phase matching, energy and momentum conservation laws must hold for the incoming and outgoing photons. Energy conservation means that two photons with frequency ω in the incoming waves produce one photon with frequency 2ω in the outgoing wave. Momentum conservation is illustrated in fig. 8. It dictates that when the incoming ω frequency waves propagate in different directions, the second harmonic wave will be generated in the direction represented by the vector sum of the incoming photon momenta (fig. 8B); if the incoming waved differ in both frequency and direction, the sum frequency field will be emitted in the direction that can be calculated by adding their wave vectors and taking their lengths into account (fig. 8C).

Using crystals one can obtain not only the second, but also higher harmonics of the laser radiation: third, fourth, etc. The third harmonic can be generated by mixing first and second

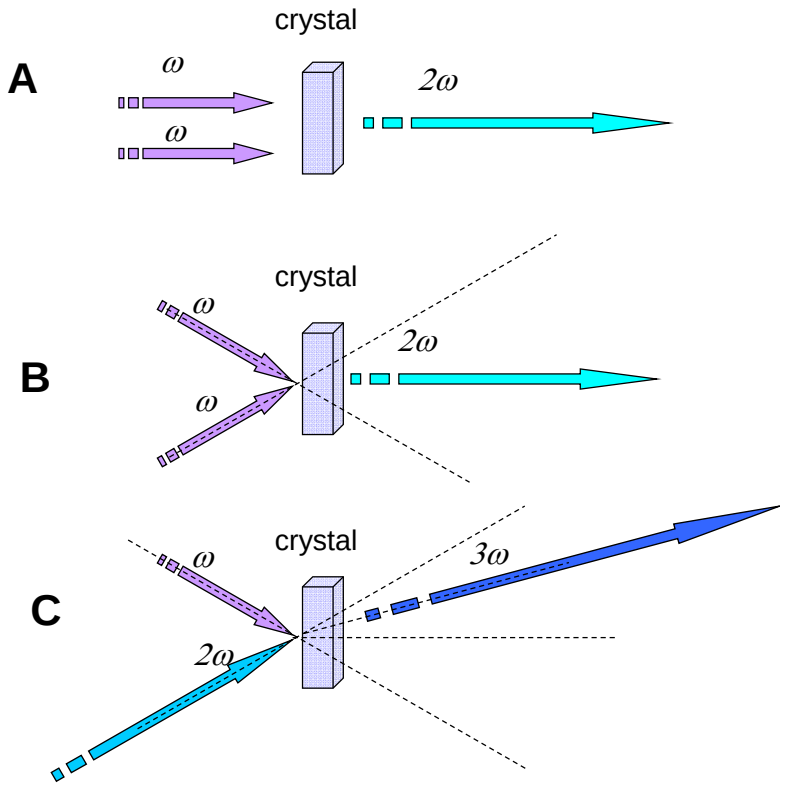

Fig. 8. Momentum conservation in harmonic generation processes. A: collinear second harmonic generation, the direction of second harmonic wave is the same as that of the incoming waves; B: non-collinear second harmonic generation, when the second harmonic is directed in the middle between the directions of the incoming waves; C: sum frequency generation, mixing waves with frequencies ω and 2ω. The direction of 3ω field is given by the vector sum of the incoming waves.

harmonic waves, and the fourth – by doubling the frequency of the second harmonic (or adding the first and third, but this is technically more complicated). These processes allow easily (one only needs a suitable crystal) extending the range of accessible laser frequencies. As the efficiency of each frequency conversion process is lower than one, some energy is always lost in the process, however, with optimum conditions, harmonic generation efficiencies of tens of percent can easily be achieved. The amount of produced light is then enough for performing time-resolved experiments.

Self-phase modulation and white light generation

As mentioned above, isotropic materials have zero second order (quadratic) dielectric susceptibility. In those materials, the first nonzero nonlinear term in eq. (9) is cubic nonlinearity. One of the phenomena pertaining to this nonlinearity we have already discussed: it is optical Kerr effect, or self-focusing used in Kerr lens mode locking. Its basis is the nonlinear refractive index described by the eq. (8). The same dependence of refractive index on light intensity is the cause of *white light supercontinuum generation*, an effect widely used in time-resolved spectroscopic experiments. The physical basis behind this phenomenon is the fact that (nonlinear) refractive index is one of the factors in the phase of the electric field (eq. (10)): wave vector k is proportional to the refractive index. This implies that the wave propagating in the medium will experience a phase shift (phase modulation) dependent on the intensity of its own electric field. Phase modulation is indistinguishable from frequency modulation, because frequency can be defined as time derivative of the phase. Thus the wave propagating in the medium with cubic nonlinearity is *self-focusing* and *self-phase modulating.* These phenomena, along with a number of other non-linear optical phenomena, broaden the spectrum of a femtosecond pulse propagating in nonlinear medium: from transform-limited pulse, a pulse of *white light supercontinuum* is generated, the spectrum of which

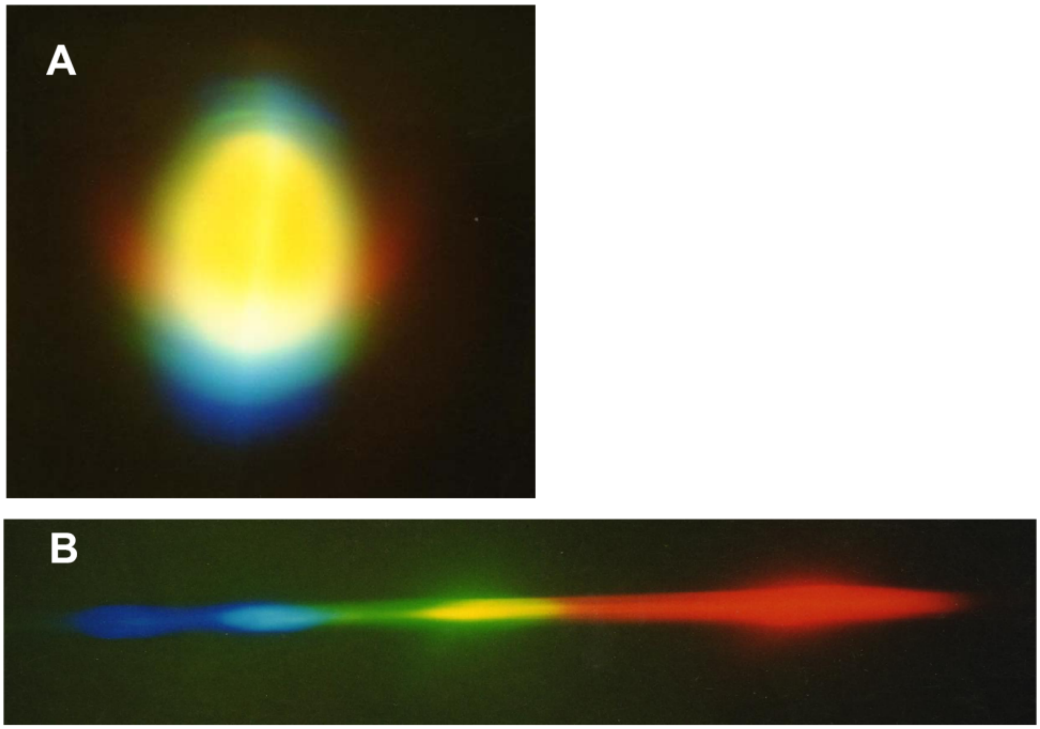

Fig. 9. White light generation in sapphire crystal. A: beam color after passing the crystal. B – the spectrum of the same beam spread out using diffraction grating and covering the entire visible range.

can cover several hundreds of nanometers. White light continuum can easily be produced by focusing high energy Ti:Sapphire laser pulses in glass or water: 800 nm light turns into white broadband radiation (fig. 9). Even though the intensity of light produced in this manner is rather low at each particular wavelength interval, white light generation is very important for time-resolved spectroscopy: supercontinuum pulses are used as probe light in pump-probe spectroscopy (see below), and they also serve as seed light in optical parametric amplifiers discussed in the following section.

Optical parametric generation and amplification

Optical parametric generation is another quadratic nonlinear optical phenomenon and observed in crystals without the center of inversion. It is, in essence, the reverse of sum frequency generation: in this case a single photon from the pump wave is split into two photons (fig. 10). The resulting wave of higher frequency is called *signal wave,* whereas the one with the lower frequency is termed *idler wave.* In general, the two produced photons have different frequencies and their frequencies, wavelengths and momenta follow the conservation laws:

$$\omega_{pump} = \omega_{signal} + \omega_{idler}$$

or

$$\lambda_{pump} = \frac{1}{\frac{1}{\lambda_{signal}} + \frac{1}{\lambda_{idler}}}; \qquad (12)$$

$$\mathbf{k}_{pump} = \mathbf{k}_{signal} + \mathbf{k}_{idler}$$

The most important and useful feature of the parametric generation is the fact that the division of frequencies (or photon energies) between the signal and idler wave depends on the phase matching condition, or, in other words, crystal orientation. This allows converting a given pump wave into a signal wave *of desired frequency*, simply by rotating the crystal to an appropriate angle, which is especially convenient for producing the tunable light source for time-resolved spectroscopy.

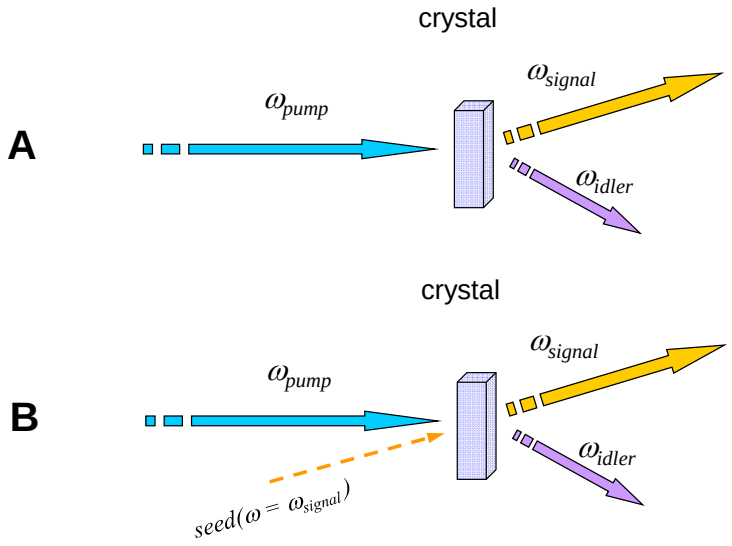

Fig. 10. A: Optical parametric generation: nonlinear crystal splits a pump photon into two different energy (frequency) photons. This process is subject to energy and momentum conservation laws. B: optical parametric amplification: seed light matching the characteristics of signal wave is applied on the crystal. It is amplified as the pump wave transfers its energy to it.

Optical parametric generation in the crystals occur when the initial photons of signal or idler waves are produced from quantum noise in the nonlinear medium and is further amplified by the pump wave. Noise is unreliable stuff, therefore, the efficiency and stability of parametric generation improves significantly, when, along with the pump wave, one applies a weak wave of desired signal wavelength to the crystal – the crystal has something to amplify from the very beginning. Here, white light supercontinuum comes in useful again: it contains all the frequencies, therefore, it serves as a perfect seed source: by directing it into the crystal together with the pump wave and rotating the crystal to an appropriate angle, one can obtain stable and strong parametric light of desired wavelength (fig. 10B).

2.1.6. Characterization of ultrashort pulses

Until now, we were concerned about the ways of producing ultrashort light pulses required for time-resolved spectroscopy. In this section, we will discuss how to determine the most important parameters of such pulses. Two most important parameters of the pulse that are of interest to the experimentalist are its frequency spectrum and duration. Measuring frequency spectrum of an ultrashort light pulse is no different from measuring the spectrum of continuous source, such as a lamp: one only needs to direct the light into a spectral instrument with dispersive element (prism or diffraction grating) and record the spectrum using a photodetector. Current spectrometers usually

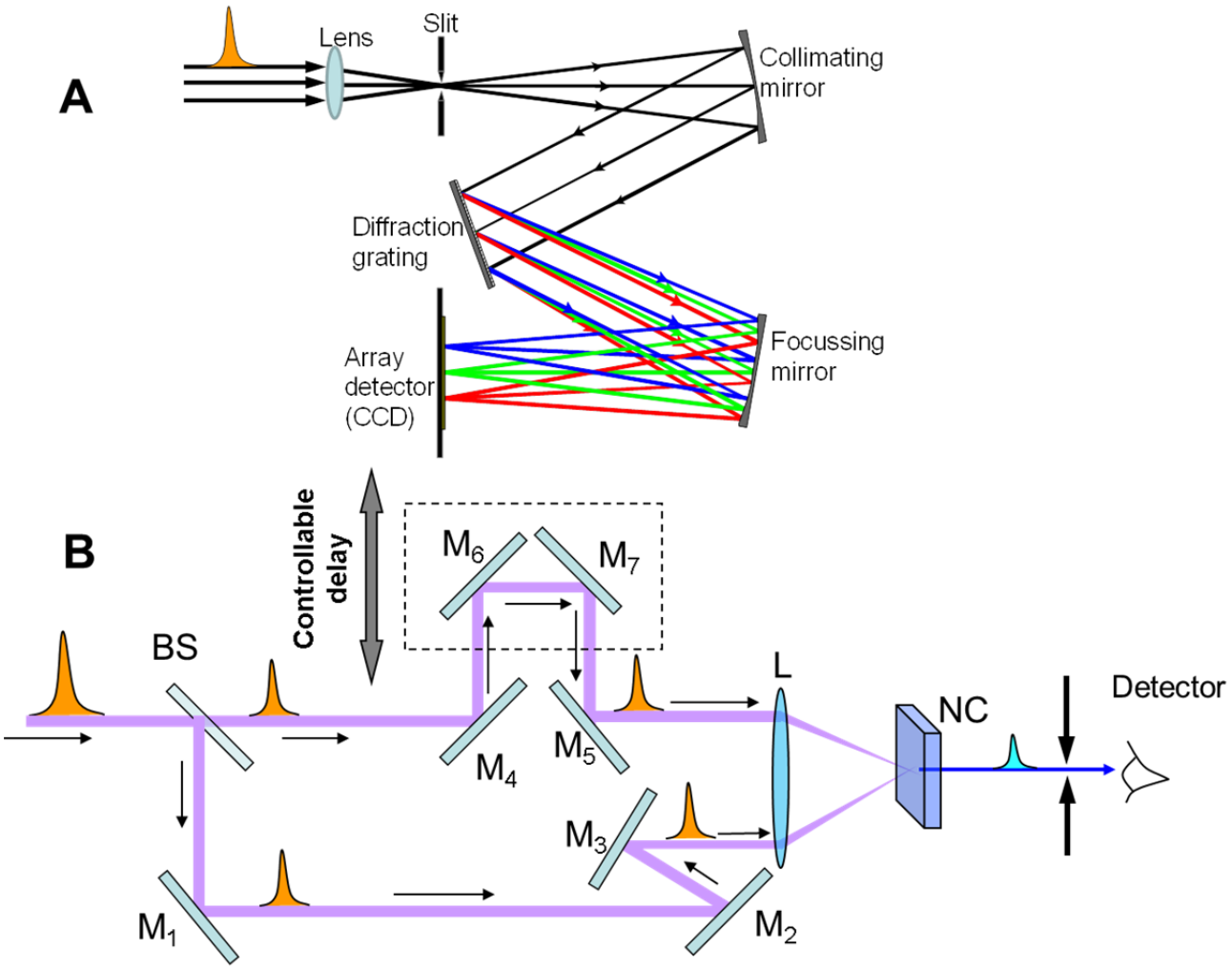

Fig. 11. Characterization of ultrashort pulses. A: Measurement of pulse spectrum using Czerny-Turner type spectrograph. B: Autocorrelator for measuring pulse duration. BS – beamsplitter, M – mirrors, NC – nonlinear sum frequency crystal. Mirrors M_6 and M_7 are mounted on a translation stage and act as a variable delay line.

employ CCD arrays, similar to the sensors of digital cameras. The scheme of such measurement is depicted in fig. 11A).

The duration of the pulse is trickier: it is in the range of tens of femtoseconds. The only available tools to measure such fast events are the ultrafast pulses themselves; therefore they must become their own measurement instruments. The simplest method of determining the duration of a femtosecond pulse is depicted in fig. 11B). The technique is called *autocorrelation*, whereas the device, the optical layout of which is shown in fig. 11B) is termed *autocorrelator*. The principle of operation involves a semitransparent mirror that splits the pulse into two replicas, one of which can be delayed with respect to the other. The delay is accomplished by spatially moving two mirrors reflecting the beam (these mirrors are mounted on a precise translation stage). The moving mirrors

together with the translation stage are termed an *optical delay line*. After traveling their respective distances, both pulses are intersected in a nonlinear crystal, where non-collinear second harmonic generation takes place, similarly to the one shown in fig. 8B. To measure the *autocorrelation function*, one needs to record the dependence of the generated second harmonic intensity on the position of the delay line. Non-collinear second harmonic generation is only possible when both pulses overlap both in time (arrive to the crystal at the same instance) and in space (spot on the crystal). If the pulses hit the same spot, by moving the delay line we can measure the second harmonic intensity proportional to the temporal overlap integral of the two pulses. To find the second harmonic intensity as a function of time *t*, we take multiply the intensities of both moving and stationary pulses and integrate over the entire time range:

$$AC(t) = \int_{-\infty}^{+\infty} I_1(\tau) I_2(t-\tau) d\tau \tag{13}.$$

Both pulses are identical – they are replicas of the initial pulse produced by the beamsplitter. With that in mind, the intensity of the second harmonic signal is

$$AC(t) = \int_{-\infty}^{+\infty} I_1(\tau) I_1(t-\tau) d\tau \tag{14}.$$

Such integral in statistics is called a temporal autocorrelation function of a time-dependent quantity. Hence the terms autocorrelation and autocorrelator. Plugging the envelope of a Gaussian pulse (2) into eq. (14) and performing the integration reveals that an autocorrelation of a Gaussian pulse is also a Gaussian function, and its width is $\sqrt{2}$ times the width of the pulse:

$$\tau_{pulse} = \frac{\tau_{autocorrelation}}{\sqrt{2}} \tag{15}.$$

Note that if we cross-correlate two different pulses, one of which is many times shorter than the other, eq. (13) will yield

$$AC(t) = \int_{-\infty}^{+\infty} I_1(\tau) I_2(t-\tau) d\tau \approx \int_{-\infty}^{+\infty} I_1(\tau) \delta(t-\tau) d\tau = I_1(t) \tag{16}.$$

In other words, the generated second harmonic pulse is proportional to the intensity of the slowly varying signal at the time instance, when the short pulse arrives. To put it simply, an extremely short pulse can be used to ‘time-slice’ the long pulse thereby directly establishing its time course. This

insight is the basis of time-resolved spectroscopic technique called fluorescence upconversion, discussed in the further sections.

With both spectral width and time duration of the pulse known, we can compute their time-bandwidth product and see how far our pulse is from the perfect Gaussian. In practice, the product is usually higher than 0.441, i.e. the pulses are not exactly Gaussian-shaped. Nevertheless, the product is often cited as one of the pulse quality parameters.

Let us note that neither autocorrelation, nor spectrum, nor both of them provide the full information about the pulse. The full information is complex function describing electric field in time (in addition to that, there is also the distribution across two transverse spatial coordinates). We have simply assumed Gaussian time shape and spectrum and discussed how to measure them both. In many cases, this information is sufficient. When full description of the pulse field is necessary, other, more complex pulse characterization methods are employed, including FROG, SPIDER, GRENOUILLE etc. [6].

3. Time-resolved fluorescence

3.1. Time-resolved fluorescence: techniques

One of the ways for a molecule to lose its excited states is fluorescence. Steady-state fluorescence spectroscopy concerns itself with emission and fluorescence excitation spectra as well as fluorescence anisotropy. The steady-state fluorescence spectrum represents the fluorescence intensity integrated over time (for the sake of discussion, let us assume that the sample is excited by a short laser pulse arriving at t=0):

$$F_{steady-state}(\omega) = \int_0^\infty F(\omega, t)dt \qquad (17).$$

In other words, the detector adds up all the photons emitted by the sample molecules, starting with the instance of excitation and ending with the time when the last excited molecule has decayed to the ground state. Eq. (17) shows that a steady-state fluorescence measurement carries no information on how and when the excited state of a molecule was deactivated. For example, two molecules may have identical fluorescence intensity, even though one of them is radiating strongly for a short time, whereas the other one glows weakly for a long time. Similarly, there is no way of interpreting steady-state measurements in order to establish what is going on with the molecule in the excited state or how the excited state is deactivated.

Time-resolved spectroscopy does not integrate the signal in time, and therefore carries the information about the molecular processes in the excited state. These processes may involve:

- Radiative relaxation (molecule emits a photon and returns to the ground state);
- Internal conversion or non-radiative relaxation (molecule uses the 'ladder' of the vibrational sublevels to return to the lower electronic state;
- Intersystem crossing (molecule goes into a triplet state);
- Conformational change (e.g. trans-cis isomerization);

Only gas-phase molecules can be thought of as completely isolated; in condensed biological matter, they are always surrounded by other molecules, such as proteins, water, lipids etc., therefore there are several more processes influencing excited state dynamics:

- Excitation energy transfer to a neighboring molecule;

- Solvation (regrouping of the solvent molecules to accommodate the excited-state electronic configuration of the molecule);
- Photoinduced intermolecular reaction, such as proton or electron transfer from the excited molecule to the solvent or a neighboring molecule.

All these processes (and more) influence the state of the molecule, and hence its fluorescence spectrum. These influences can therefore be studied using time-resolved fluorescence. In time-resolved fluorescence spectroscopy, the molecules are usually excited using a laser pulse and their fluorescence spectrum is recorded as a function of time, i.e. the measured signal can be written down as follows:

$$F = F(\lambda, t) \tag{18}$$

Here we the spectral variable is chosen to be wavelength, but frequency or wavenumber may equally well be used.

Let us examine a simplified case: the ensemble of molecules excited using a Gaussian laser

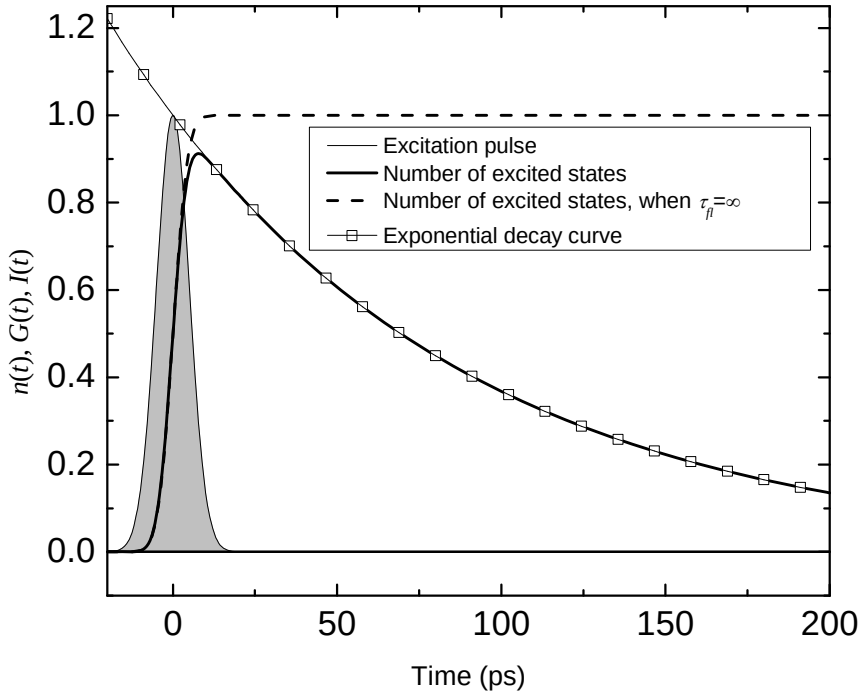

Fig. 12. Fluorescence of hyptotetical molecular sample (solid line) after the excitation by a Gaussian pulse (gray area). Fluorescence decay is shown as thick solid line. Dashed line shows the population of the excited state with no decay. Thin line with squares represents the exponential function describing the decay of excited states (eq. (20)).

pulse $I(t) = \frac{1}{\sqrt{2\pi}\tau} e^{-\frac{t^2}{2\tau^2}}$ (gray area in fig. 12), and the only channel for the molecule to lose its excited state is fluorescence (emission of a photon). Further, we assume that the excitation pulse is not so intense as to saturate the excited state population via stimulated emission. In this case, the number of molecules in the excited state is described by the following differential equation:

$$\frac{dn}{dt} = \frac{A}{\sqrt{2\pi}\tau} e^{-\frac{t^2}{2\tau^2}} - \frac{1}{\tau_{fl}} n \qquad (19),$$

where A is the amplitude of the excitation pulse, τ_{fl} – is the fluorescence lifetime of the excited state (the reciprocal of fluorescence rate).

The solution of homogeneous equation corresponding to eq. (19) is the decaying exponent $Ce^{-\frac{t}{\tau_{fl}}}$ (thin line with squares in fig. 12). By varying the constant and using the initial condition $n(t = -\infty) = 0$ we can also find a general solution, the graphical representation of which is given in fig. 12 by a solid black line. It is the product of two factors:

$$n(t) = G(t) \cdot e^{-\frac{t}{\tau_{fl}}} \qquad (20)$$

G(t) has no expression in elementary functions, however, it is proportional to an integral of a Gaussian pulse envelope over the range from $-\infty$ to *t*. It can be written down in terms of error function *erf*(*t*):

$$G(t) \sim 1 + erf\left(\frac{t}{\tau}\right)$$
$$erf(t) \equiv \frac{2}{\sqrt{\pi}} \int_0^t e^{-t^2} dt \qquad (21).$$

Its graphic representation is shown in fig. 12 (dashed line), and the physical meaning is intuitively clear: this is how the number of the excited states in the sample would vary, if the fluorescence lifetime τ_{fl} were infinitely long (thereby making the exponential function in eq. (20) equal to one). Naturally, the number of excited states in the sample is then proportional to the number of photons that have entered the sample until the time *t*, i.e. the integral of the pulse envelope in the range from $-\infty$ to *t*.

The observable fluorescence intensity at each time is proportional to the number of molecules in the excited state. Therefore, eq. (20) tells us that the fluorescence of our hypothetical

sample will increase following the integral of the pulse envelope, and subsequently decay in an exponential fashion. It is important to note that at time instances much later than the duration of the excitation pulse, the decay of fluorescence is exponential and all the subtleties pertaining to the excitation pulse can be neglected (compare squares and the solid line in fig. 12). This is only the case when the excitation pulse is much shorter than the fluorescence lifetime.

So far, our model did not include any processes affecting the fluorescence spectrum of the sample, therefore, the spectral shape in this case will remain constant, only the intensity will decay with time, according to the eq. (20). This, in a way, is boring – the spectral degree of freedom does not carry any interesting information. In the examples that follow, we will see that the spectral shape changes are of special interest, because they allow us to draw conclusions about the physical processes occurring in the sample during its excited state lifetime.

But before we do that, we will devote the following section to discuss the experimental techniques of measuring time-resolved fluorescence spectra (18). We can divide these techniques into electronic (where fast electronic detectors are used to record fluorescence) and optical, where nonlinear optic tricks are used, similar to the one we discussed while describing pulse autocorrelation measurements.

3.1.1. Time-correlated single photon counting

This electronic method is useful, when excitation is performed using high repetition rate lasers (e.g. Ti:Sapphire oscillator). After excitation of the molecule by a laser pulse, it will sit in the excited state for some time, and eventually, after time Δt, it will emit a photon. If we find a way of measuring Δt multiple times (i.e. exciting the molecule with a large number of laser pulses), the obtained waiting time values will be distributed according the probability of the radiation at particular time. This insight is employed in time-correlated single photon counting (TCSPC) experiment, the principle of which is illustrated in fig. 13. High repetition rate laser is firing ultrashort pulses into the sample. Part of the laser light is split off by a beamsplitter and directed to a fast photodiode, creating an electrical pulse. This pulse further goes into a discriminator that converts this pulse of unknown temporal shape into a digital ‘start’ signal. Start signal is used to start a time-to-voltage, or time-to-amplitude converter (TAC). TAC is a device that produces an analogue voltage signal proportional to the delay between two digital electronic pulses (‘start’ and ‘stop’). It is, in essence, just a capacitor charged by a constant current, or ramp generator. Fluorescence photon

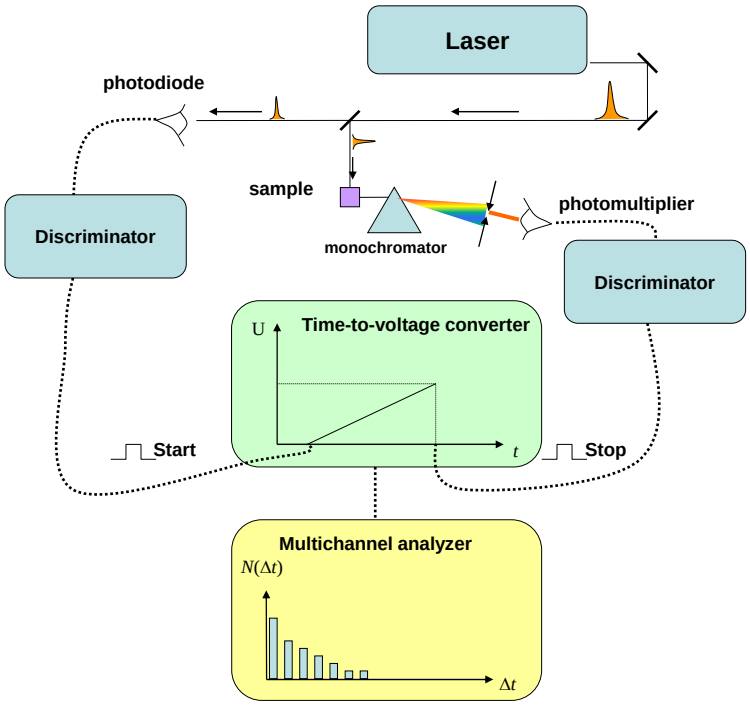

Fig. 13. The principle of time-correlated single-photon counting: laser pulse is split into two, one of which starts the time-to-voltage converter, whilst the other is used to excite the sample. The converter starts to accumulate the signal and proceeds until it is stopped by the signal of fluorescence photon emitted by the sample (the photon is recorded by a photon-counting photomultiplier). The voltage corresponding to the duration between the photodiode (start) and photomultiplier (stop) pulses is recorded by the multichannel analyzer. After repeating experiment multiple times, a histogram representing the fluorescence decay is measured.

emitted by the sample is captured by a sensitive photomultiplier (PMT), the signal of which is also processed by the discriminator and directed to the TAC as a 'stop' signal. As a result, TAC ends up holding a voltage, proportional to the duration between 'start' and 'stop' photon, or, in other words, the period of time between excitation and emission. This voltage is stored in a multi-channel analyzer – a device consisting of a series of counters, one of each is incremented every time a voltage signal is received. The number of counter incremented corresponds to the observed voltage: e.g. if the voltage is between 0 and 0.1 V, counter No.1 is incremented, if it is between 0.1 and 0.2V – counter No.2 is incremented, and so forth. (Technically, this can be realized by converting the analog voltage into an integer number using an ADC. The obtained number is used as an address of RAM, the number at which is incremented).

This way, a fluorescence decay histogram is recorded: the counters corresponding to often observed delay times between the excitation and emission accumulate highest numbers (they are incremented very often), whereas the counters corresponding to seldom occurring delays see just a few photons.

TCSPC is an electronic method, and its main disadvantage is a limited time resolution. Note that it is not, in fact, limited by the response time of the detectors (photodiode, PMT): the discriminators do not register the response itself, but rather fire their electronic pulses when the signal of the detector reaches a predefined percentage of the maximum. This way picosecond and nanosecond time resolution is accessible, even if the response of the detector to a light pulse is several microseconds (the only requirement for it being the *reproducibility* from pulse to pulse). The measurement uncertainty comes from so called 'jitter', i.e. differences of signal shape from one pulse to another. In practice, TCSPC allows the time resolution of around 50 ps. Time resolution of TCSPC (and other time-resolved fluorescence experiments) is usually measured by measuring the duration of light pulse elastically scattered by the sample. Scattering is an instantaneous process and its temporal shape is determined only by the time-response of the instrument.

Another disadvantage is the fact that TCSPC is, in essence, a single-wavelength method. At each given time, fluorescence kinetics is only registered at one detection wavelength. To register the entire spectrum, one either has to measure different kinetics sequentially, or buy more detectors and *all* the electronic components, which is an expensive solution.

However, TCSPC has important advantages: it does not require intense excitation light. In fact, it is bad if the excitation pulse energy is too high. The underlying assumption of the method is that each excitation pulse causes only one fluorescence photon to be detected. TCSPC is also completely insensitive to the stability of the laser pulse energy (even if these energies fluctuate by the factor of two, the method still works). You can actually switch off the laser in the middle of the experiment, wait for half an hour and then continue as if nothing has happened. The measurement is cumulative, i.e. one can count photons until the desired signal-to-noise ratio is reached, and the quality of the data allows answering the question posed by the experimenter.

Compared to the other time-resolved spectroscopic methods, TCSPC is cheap. It became popular after the advent of diode lasers providing laser pulses in the 100 ps range. Such lasers cost only a few percent the price asked for a 'real' ultrafast system. TCSPC has also been applied in fluorescence lifetime imaging, where fluorescence recorded by a confocal microscope is also measured with time resolution. Thereby, each pixel of fluorescence image also contains a fluorescence decay information [7].

3.1.2. Streak camera

Streak camera is another method of measuring time-resolved fluorescence. Its principle slightly resembles the operation of old-fashioned analog oscilloscope, and the operation scheme is depiced in fig. 14. It consists of three stages.

- Fluorescence photons from the sample knock out electrons from photocatode.
- Electrons are accelerated in an electric field, after which they enter the space with fast-varying sweeping electric field. In this manner, the arrival time of the electrons (or, ultimately, photons) is converted into position of electron beam in space.
- Deflected electrons hit the phosphor screen, producing the image, which is recorded by the CCD camera. From the position of the electron flashes on the screen, their arrival time can be estimated.

Thus, in streak camera, photons are converted into electrons, whose arrival time is converted into spatial coordinate by the sweeping voltage (electrons that arrive later find a higher voltage on the

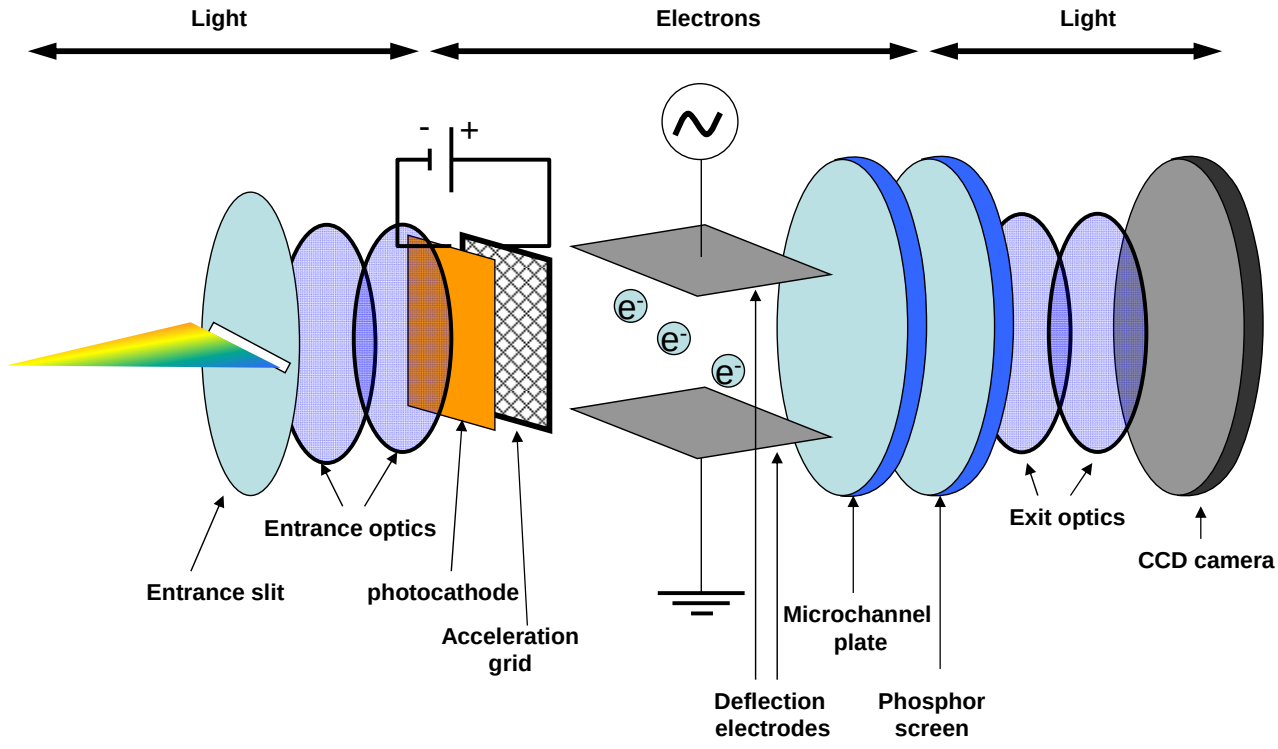

Fig. 14. Operation of a streak camera. Fluorescence photons knock out electrons from photocatode. The electrons are accelerated in an electric field and enter the space between deflection electrodes, to which a fast-varying sweeping voltage is connected. Sweeping voltage converts the time of arrival of the electrons into position in space. The start of the sweep is synchronized with an excitation laser pulse. Deflected electrons hit the phosphor screen, the image on which is registered by a CCD camera.

deflection plates and are displaced more). Subsequently, the electron distribution is converted back into the distribution of light (image) on the phosphor screen. To increase sensitivity, the electron image is usually amplified by a microchannel plate PMT, placed before the phosphor. The image is detected by a sensitive CCD camera.

The main advantage of a streak camera compared to the other fluorescence techniques is the fact that deflection plates use only one spatial direction (vertical in fig. 13). The remaining spatial coordinate can therefore be used for spreading the spectrum by a spectrograph. Thus, the entire two dimensional (spectro-temporal) data is collected in a single experiment. Additionally, streak camera is faster compared to TCSPC, because it is based on a simple vacuum tube. Typical time resolution of a syncroscan[3] screak camera can be down to 1 ps. Given the fact that this is the resolution of the *entire* time-resolved fluorescence spectrum (eq.(18)), the speed of data collection with streak camera exceeds TCSPC by a large margin (and, of course is more expensive by more or less the same margin).

3.1.3. Fluorescence upconversion

This technique of time-resolved fluorescence spectroscopy is based on nonlinear optical tricks rather than cutting-edge electronics. The experimental layout of upconversion experiment, shown in fig. 15, resembles the autocorrleator (fig. 11B). To obtain fluorescence signal from the sample, the sample is placed into one of the branches of the autocorrelator and cross-correlation between the excitation laser pulse and sample fluorescence is recorded, by adding the frequencies of both light pulses in the nonlinear crystal. More specifically, the pulse from the laser is split into two, one of which is delayed in the optical delay line (it is called gating, or gate pulse). The rest of the light is used (usually after additional devices to produce the correct excitation wavelength) to excite the sample. The emitted fluorescence is collected using off-axis parabolic (or elliptical) reflectors or lenses and is focused into nonlinear crystal [8]. Mirrors instead of lenses are used to get the best time resolution, because they do not introduce additional dispersion in the signal. Gate pulse is overlapped in the crystal with the fluorescence pulse. Crystal orientation is chosen to satisfy the

[3] Synchroscan is a type streak camera that allows accumulating data from multiple laser shots on the CCD. This type of camera is many times more sensitive than single-shot streak cameras; however, the jitter in the synchronization circuitry slightly ‘smears out’ the time response.

phase matching condition for sum frequency generation between the gate and the emission wavelengths.

Sum frequency generation is a quadratic nonlinear optical phenomenon (see above), and the intensity of resulting sum frequency is proportional to the product of intensities of the two added fields:

$$I_{upconv}(t) \sim I_{gate}(t) \times I_{fluorescence}(t) \quad (22).$$

Therefore, if the gate pulse intensity is kept constant, the measured signal is proportional to the fluorescence intensity of the sample *at the time instance when sample fluorescence is overlapped with the gate pulse* (fig. 16). In other words, the short gating pulse cuts time slices out of long fluorescence pulse. These slices are registered by the detector as time-frozen fluorescence intensities. The instance, at which they are frozen, depends on the delay of the gating pulse. This implies that varying this delay allows recording fluorescence intensity as a function of time. The frequencies of fluorescence and gate pulses are added in the nonlinear crystal; therefore, with the wavelength of gate pulse known, one can recover the fluorescence wavelengths using equation

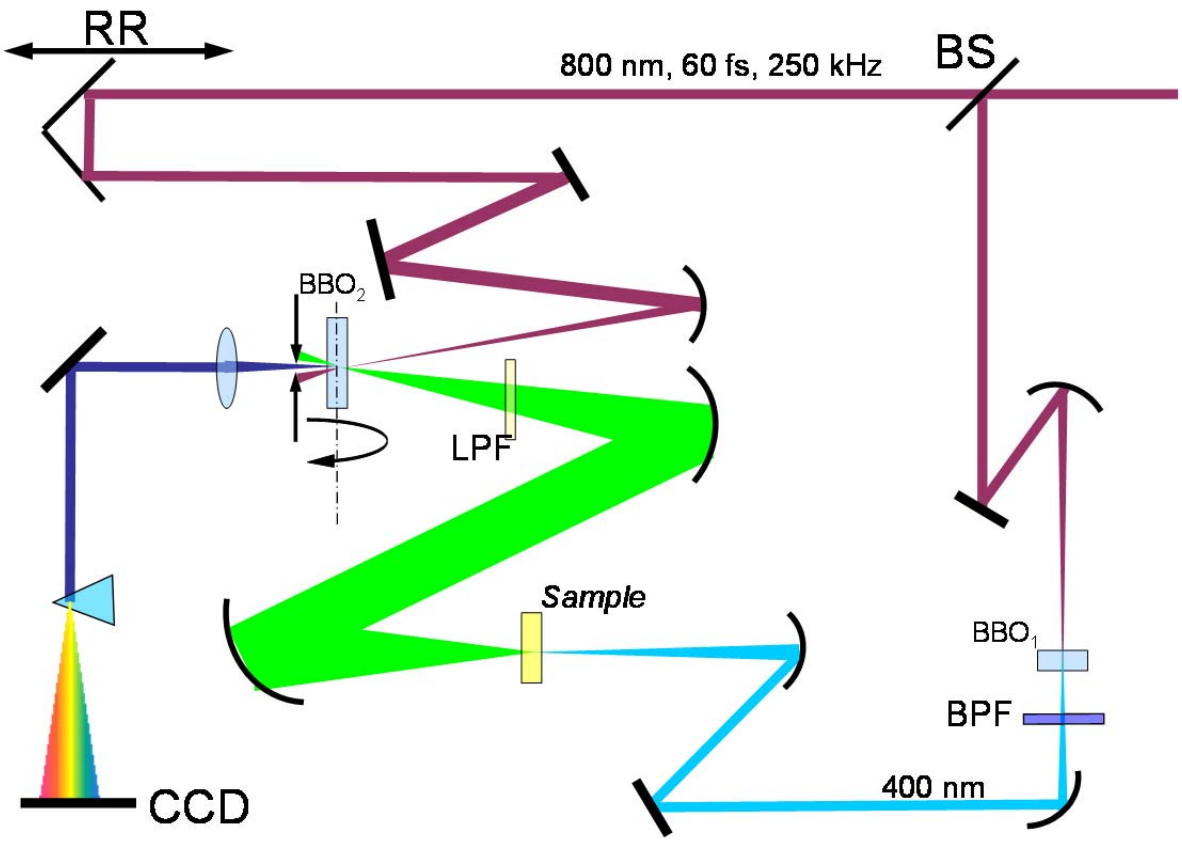

Fig. 15. Fluorescence up-conversion experiment: the pulse is split into two, one of which (gate) is delayed by the optical delay line, whereas the other is used (after second harmonic generation in BBO_1) to excite the sample. The fluorescence emitted by the sample is collected using off-axis parabolic reflectors and focused into a nonlinear crystal BBO_2 together with the delayed gate pulse. BBO_2 generates sum frequency between the gate and the fluorescence, the spectrum of which is spread by the monochromator and recorded by the CCD detector.

$$\frac{1}{\lambda_{recorded}} = \frac{1}{\lambda_{fluorescence}} + \frac{1}{\lambda_{gate}} \qquad (23),$$

because the wavelength of the recorded signal is measured experimentally.

Fluorescence upconversion is a purely optical method, and its time resolution is essentially limited only by the pulse duration of the employed laser pulses. This resolution can easily be 150 fs and less, when Ti:Sapphire lasers are used as excitation and gate light sources. Therefore, fluorescence upconversion is the method of choice, when the investigated processes are extremely fast (faster than 1 ps). Other methods cannot compete for time resolution. However, there are also disadvantages. Frequency upconversion (sum frequency generation) is a nonlinear process, necessitating the use of intense excitation pulses, often damaging to biological samples. Due to the uncertainties of phasematching condition, different upconversion efficiencies at different wavelengths and other subtle nuances that are hard to control during the experiment, it is tricky to

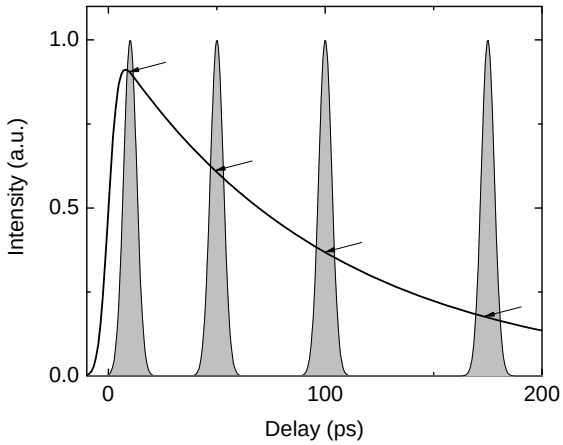

Fig. 16. Fluorescence upconversion: a long pulse of sample fluorescence is sliced in time by a short gating pulse with controlled delay in a nonlinear crystal. The registered signal (arrows) is proportional to the fluorescence intensity at the moment of gate pulse arrival.

measure undistorted fluorescence spectra when using upconversion technique. Finally, this technique only records fluorescence at a single time point and a single spectral point. To get spectro-temporal data, one has to scan both wavelength and delay, which takes time.

3.1.4. Optical Kerr shutter

This method is essentially a different version of fluorescence upconversion: the general idea of the experiment is the same, with the exception that a different nonlinear optical effect is used for time slicing. The effect in question, as name suggests, is optical Kerr effect. This is a phenomenon, when isotropic material (water or fused silica) becomes birefringent when placed in a strong linearly polarized light field. Birefringence means that the polarization of linearly polarized light traversing

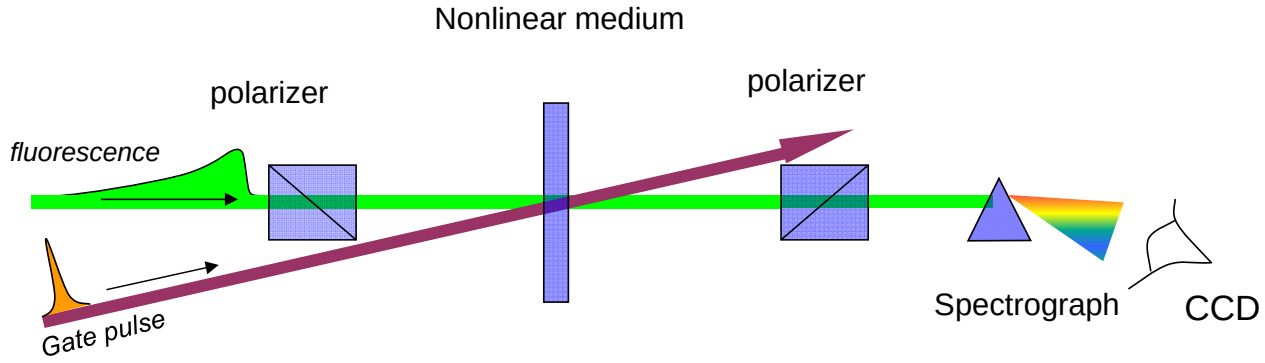

Fig. 17. Optical Kerr shutter: fluorescence is allowed to pass the optical train consisting two crossed polarizers and a nonlinear medium. When the gate pulse impinges on the medium, the polarization of the fluorescence light gets rotated and the light overlapping with the gate pulse is transmitted through the second polarizer.

the material is partly rotated.

The optical layout of such experiment is shown in fig. 17. Fluorescence light is allowed to pass the shutter consisting of crossed polarizers with nonlinear medium (fused silica window, water cell or carbon disulphide cell ar the usual choices). When the gate pulse is absent, the medium is isotropic, there is no birefringence and the fluorescence is blocked by the second polarizer. When the gate pulse arrives, polarization of the fluorescence light, created by the first polarizer, is rotated due to optical Kerr effect, and some of the light is transmitted through the second polarizer to be dispersed in a spectrograph and detected by a sensitive CCD. Similarly to fluorescence upconversion, the signal arises only from the part of fluorescence pulse overlapping in time with the gate pulse.

The advantages and drawbacks of this method are similar to those of fluorescence upconversion. However, the added advantage of Kerr shutter is the fact that the frequency of fluorescence light is unaffected – we directly measure the intensity of sample fluorescence. As a disadvantage, we note that optical Kerr effect is the third order nonlinearity. This is both good and bad: good because phase matching is not important. Bad, because the gate pulse intensities required for it to occur are enormous. The liquids with relatively high Kerr nonlinearities (water and CS_2) feature a non-instantaneous (dipolar) response, limiting their time resolution to several picoseconds.

It must be noted that the time-resolved fluorescence methods based on the tricks of nonlinear optics are not easy: one needs high gate pulse intensities, sensitive detectors and very high-quality optical components for rejecting unwanted light and transmitting the light to be measured.

3.1.5. Phase fluorimetry: time resolution obtained in frequency domain

Phase fluorimetry, or frequency domain time-resolved fluorescence spectroscopy is, perhaps, the oldest among time-resolved fluorescence techniques. Despite its age and drawbacks, the method is very useful, when large batches of samples need to be characterized quickly. It does not require pulsed lasers. An incoherent light source, a couple of monochromators and a detector is all you need, therefore, this method is – at least, in principle – the cheapest. It is based on the following brilliant insight: fluorescence light leaves the sample slightly later (in fact, on average fluorescence lifetime later) than the excitation light arrives. If we excite the sample using modulated light source (e.g. the light from the lamp will be passed through a rotating disk with holes in it), the fluorescence light will be modulated at the frequency of the excitation light, but will experience a phase shift with respect to

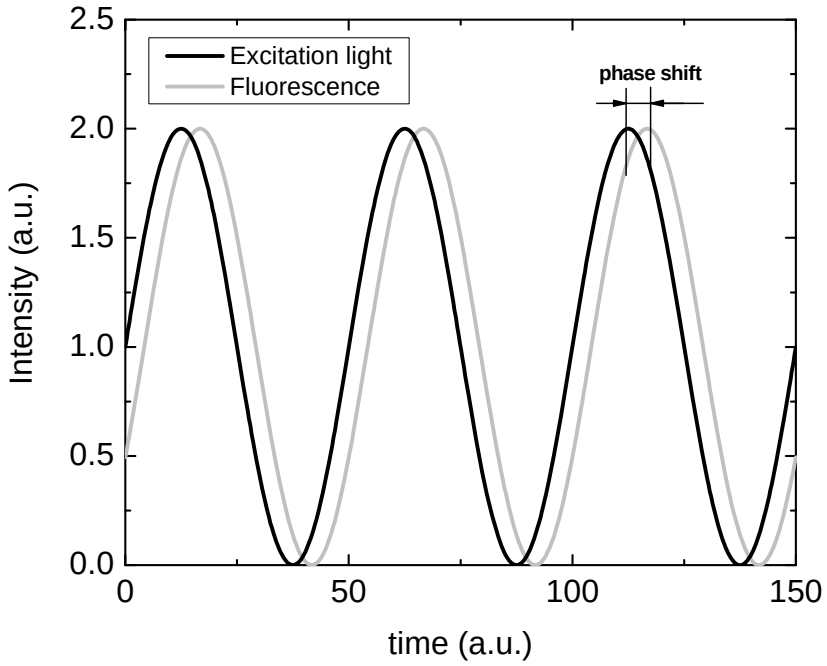

Fig. 18. Phase fluorimetry: the sample is excited using fast-modulated light (black line). Because the fluorescence takes some time to occur, the detected fluorescence light is modulated at the same frequency, and exhibits a phase shift with respect to the excitation light. From the phase shift, an average fluorescence lifetime can be calculated.

the excitation light (fig. 18). The phase shift, loosely speaking, will correspond to the delay between the excitation and fluorescence. Sensitive electronic devices called lock-in amplifiers allow very precise detection of phase shift between two signals. Assuming some shape of fluorescence decay in the sample (usually exponential decay), we use the phase shift to deduce the fluorescence lifetime (the exponent). Tricks can be done to enhance time resolution: one can sweep the modulation frequencies, or use modulation depth of fluorescence as an additional input deducing the time course of fluorescence decay. However, at the end of the day, this is a purely electronic method and picosecond-femtosecond time resolution is a challenge for it.

As already mentioned, this method is the simplest, and hence the cheapest: it does not require pulsed lasers, nonlinear crystals and other fancy laserline components. Its accuracy and reliability when pushed to the limits (picoseconds) is inferior to the direct measurement methods, because in order to determine the fluorescence decay times, we must *postulate* its kinetic shape. Direct methods do not need such assumptions; they simply measure the fluorescence decay. However, since the method is quick and accessible, it has its uses.

4. Time-resolved fluorescence: biological applications

In this section, we will discuss several biological applications of time-resolved fluorescence spectroscopy. The goal is to give worked examples of natural processes, where this technique provides new insights. To achieve those goals, we will briefly introduce the investigated systems, discuss the selected data and their biophysical interpretations. The examples include energy transfer in the photosynthetic light-harvesting complexes of bacteria, proton transfer reaction in the green fluorescent protein (GFP) of jellyfish *Aequoria victoria* and deactivation of excited state in bacterial light-driven proton pump, bacteriorhodopsin.

4.1. Excitation energy transfer in light harvesting complex LH2 of purple bacteria

Photosynthesis is the process taking place in plants, some bacteria and algae, during which almost all the energy used by all living organisms (including us) is captured and stored in the form of sugars. This process starts when light quanta are absorbed and their energy is used to separate charges across biological lipid membrane. Later, the energy of separated charges is used for synthesizing ATP and NADPH. These are further used in Calvin cycle where carbohydrates are made out of CO_2 [9]. Energy transfer and charge separation must compete with the lifetime of excited states in the photosynthetic pigments. Therefore, when the photon is absorbed, it takes only several tens of picoseconds for the energy to reach the reaction centre protein, where primary charge separation takes place. Overall quantum efficiency of photosynthesis is close to unity [10].

The photosynthetic apparatus of purple bacteria called *Rhodobacter sphaeroides* and *Rhodopseudomonas acidophila* consists of two types of light harvesting antennae and reaction center. The task of pigment-protein complexes called light harvesting antennae is to absorb light and transfer the energy of the excitation into the reaction center, where the energy is utilized for charge separation across the membrane of the cell. One of the antennae called LH2 (light-harvesting complex-2) has a three dimensional structure shown in Fig. 19. This structure is determined from x-ray diffraction on the crystal of LH2 protein [11]. Figure 19 also contains the absorption spectrum of this complex. As obvious from the figure, LH2 consists of two sets of bacteriochlorophyll pigments and a set of carotenoid pigments arranged in concentric circles. Thus the entire complex consists of nine circularly arranged subunits, each containing three bacteriochlorophylls and one carotenoid

molecule. The lowest absorption band[4] of bacteriochlorophylls in the closely packed ring (green color in Fig. 19) is at 850 nm, therefore these bacteriochlorophylls are called B850. Loosely packed bacteriochlorophyll ring absorbs 800 nm light and is called B800. The Q_x transitions of all the bacteriochlorophylls correspond to the absorption band at 590 nm. Carotenoids (elongated pigments shown in orange) absorb in the visible spectral range at 450-550 nm. They supplement the absorption spectrum of the photosynthetic apparatus and absorb the wavelengths, to which bacteriochlorophylls are transparent. Time-resolved fluorescence experiments performed by R.Jimenez and coworkers [12] helped to elucidate how energy is transferred between bacteriochlorophylls with identical and different absorption maxima.

Energy transfer from B800 to B850 can be probed by exciting B800 pigments and

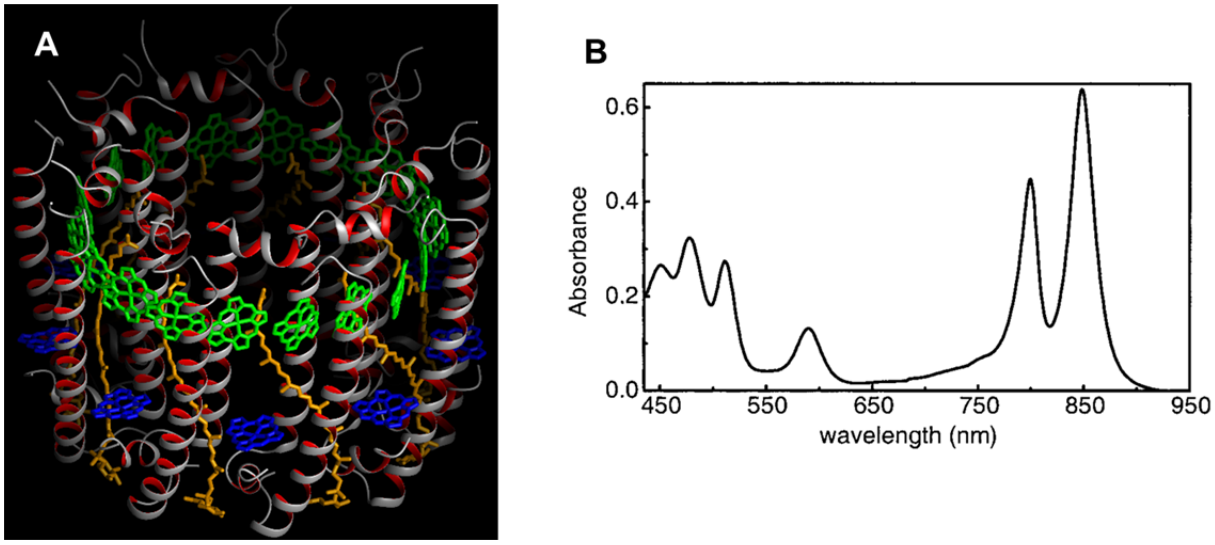

Fig. 19. Three-dimensional structure (A) [11] and absorption spectrum (B) of LH2 of *Rhodopseudomonas acidophila*. Carotenoind molecules shown in orange absorb at 450-550 nm, blue bacteriochlorophylls (B800) – at 800 nm and green bacteriochlorphylls (B850) at 850 nm. The protein is shown as helices.

monitoring the fluorescence at 900 nm. The energy will initially be located on B800 pigments, and should be transferred downhill to B850 pigments. Therefore, initial fluorescence intensity at 900 nm, where B850 pigments dominate will initially be low, and, as energy is received from B800, it should increase.

[4] In bacteriochlorophylls and other porphyrin type pigments, the lowest energy transition is called Q_y, the second-lowest is Q_x, and the transitions corresponding to the blue-violet absorption are called Soret.

The results of such experiment are shown in Fig. 20 A. As expected, immediately after the excitation of B800 pigments, the fluorescence is virtually zero (signal at t=0). However within 650 fs the signal rises and reaches its maximum. This corresponds to the energy transfer time from B800 ring of bacteriochlorophylls to B850.

So it is easy to measure energy transfer B800 → B850 in this fashion (well, not exactly easy keeping in mind all experimental difficulties and hitches that are usually left out of the scientific papers). But at least it is clear how this can be done. On the other hand, observation of energy transfer within B850 ring poses a greater challenge, because the energies of all pigments are all the same (corresponding to the energy of 850 nm photon) and energy transfer cannot be observed by selecting an appropriate detection wavelength as it was done in B800 → B850 transfer. R.Jimenez and coworkers have solved this problem by measuring the depolarization of fluorescence, i.e.

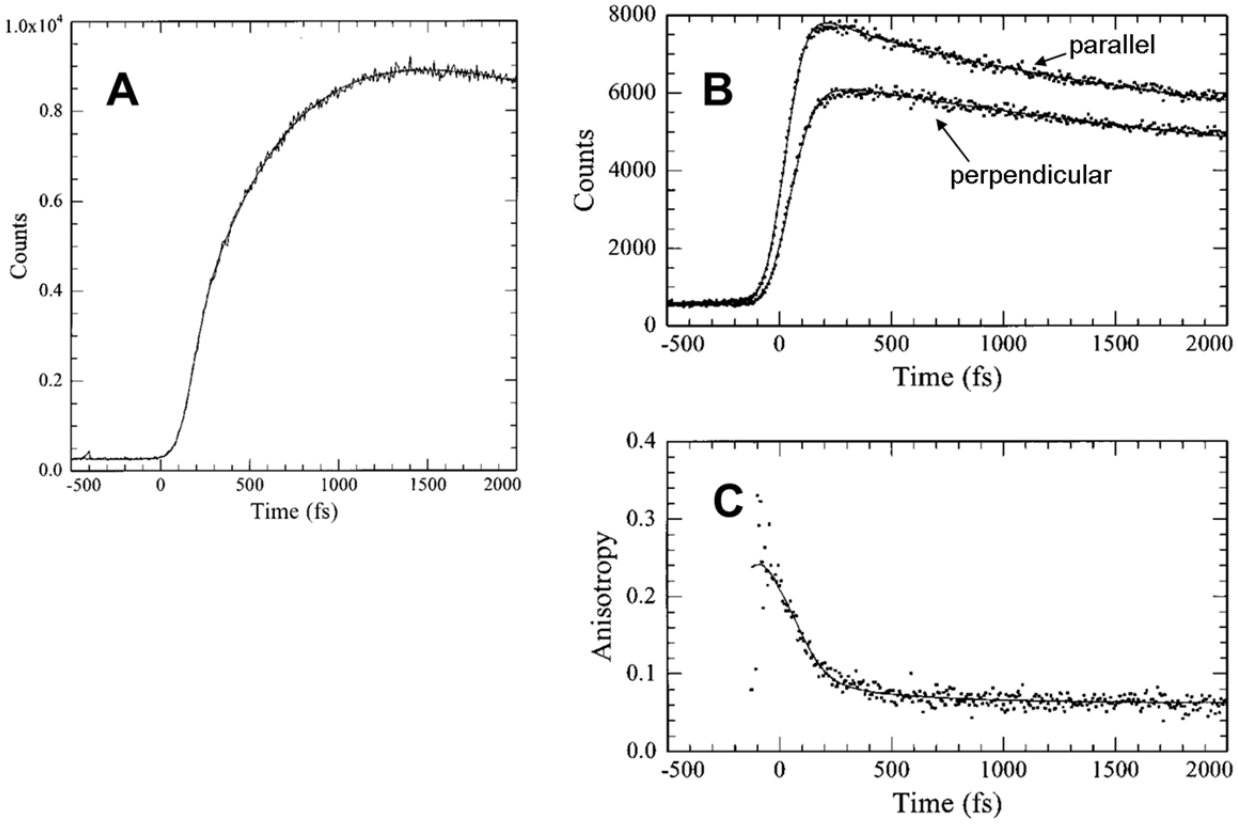

Fig. 20. Fluorescence upconversion experiments on the light harvesting antenna LH2 of purple bacteria. A: Fluorescence kinetics at 940 nm after excitation of 800 nm absorption band. B: Polarized fluorescence experiment with the excitation in B850 bacteriochlorphylls. Top curve is the measurement with detection and excitation polarizations in parallel, bottom curve perpendicular. Kinetics of fluorescence anisotropy calculated using Eq. (4.14.5). Reproduced from [12].

exciting the B850 bacteriochlorophylls and recording the fluorescence polarized parallel and perpendicular to the polarization direction of the excitation beam (Fig. 21). Fluorescence anisotropy is defined as follows:

$$r = \frac{I_{\parallel} - I_{\perp}}{I_{\parallel} + 2I_{\perp}} \qquad (24),$$

It can be shown that in the cases when fluorescence occurs from the same state that was originally excited, and the molecules are not rotating, the ensemble of randomly oriented pigments, yields fluorescence anisotropy equal to 0.4 [13]. In the context of time-resolved fluorescence, it means that initial anisotropy is *allways* equal to 0.4, because initially the emission will occur from the same pigment that was originally excited. Later different reasons may determine the depolarization of fluorescence (i.e. the directions of radiating dipoles may become different from the absorbing ones). These reasons include

- Rotational diffusion of molecules,
- Molecular changes (photoreactions) in the excited state,
- Radiationless relaxation to a different molecular state with a differently oriented transition dipole moment,
- Energy transfer,
- Etc.

We are interested in the depolarization due to energy transfer, because this is what we would like to watch in a time-resolved fluorescence experiment. It is obvious that after the hopping of excitation

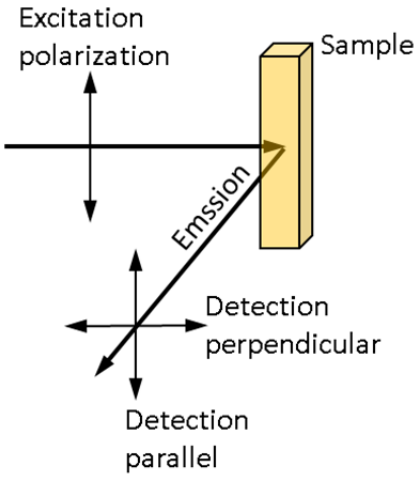

Fig. 21. Measurement of fluorescence parallel and perpendicular to the excitation polarization

from one pigment to another, with differently oriented transition dipole moment, fluorescence depolarization will occur, even if the wavelength of fluorescence remains the same. Depolarization of fluorescence recorded in LH2 B850 ring is shown in Fig. 20B, C. Panel B shows the fluorescence signal with LH2 excitation at 850 nm and detection of parallel[5] (top curve) and perpendicular (bottom curve) components at 940 nm. First, we must note that none of the curves shows ultrafast dynamics with characteristic times of 100 fs or less. However, if the measured curves are plugged into the Eq. (24) and anisotropy is calculated, femtosecond processes come unraveled. The anisotropy change is plotted in Fig. 20C. It is obvious that depolarization of B850 fluorescence is lighning-fast: instrument response function (160 fs in this experiment) is too slow to capture the initial value of 0.4, and within 200 fs, the final polarization value is established, equal to 0.06. This is an indication that the energy transfer rate in B850 ring is extremely fast.

Modelling of the fluorescence anisotropy performed by R. Jimenez and coworkers has revealed that a single hop of energy between the pair of B850 bacteriochlorophylls must be roughly 100 fs. As obvious from the final value of anisotropy in Fig. 20C, the fluorescence remains partly polarized even after a large number of energy hops. The reason for this is that a single LH2 ring contains just 18 bacteriochlorophylls, in a rigid cylindrical arrangement (see Fig. 19A), and some information about the direction of initially excited transition is retained even after the excitation is completely randomized within the ring. Losely speaking, this can be interpreted as the excitation sometimes returning to the originally excited pigment, which will re-polarize the fluorescence signal.

To conclude, polarized fluorescence experiments have answered the question that could not be addressed by isotropic experiments: they allow detecting energy transfer between isoenergetic pigments (pigments with identical transition energies), which in case of B850 ring in LH2 is 100 fs.

4.2. Proton transfer in green fluorescent protein (GFP)

Some marine organisms, such as plankton, fish and jellyfish sometimes emit light produced in their organisms via chemical reactions. The process is called bioluminescence (also commonly observed in fireflies) and the most famous organism in which it is observed is a jellyfish called *Aequoria Victoria*. It is not completely clear, why it luminesces; in fact, it rarely does, when left alone. However, it is easy to light them up by externally prodding them. It is known, that the light

[5] Terms parallel and perpendicular are defined with respect to the polarization of excitation beam.

originates in a chemically active protein called aequorin, which emits bluish light (spectral maximum at around 469 nm [14]). However, when the jellyfish is disturbed, it emits green light (508 nm). This shift in wavelength is caused by another protein called green fluorescent protein (GFP), to which the energy of aequorin is transferred and which then emits green photons. This protein is unique in the sense that it is optically active in the visible range without any prosthetic groups (pigments), such as bacteriochlorophylls or carotenoids, participating in photosynthesis. In GFP, the fluorophore is formed autocatalytically, from the primary sequence of aminoacid residues [15]. This property of GFP makes it a valuable tool of molecular biology (so valuable, in fact, that Nobel Prize in Chemistry was awarded for it in 2008). Biochemists learned to clone this protein and express it in bacteria [16]. Genetic manipulations allow fusing the gene of GFP to the gene of virtually any protein of interest and that protein is thereby marked with a green fluorescent tag, allowing optical observation of its movements within a cell or organism. For example, making a mouse mutant with epithelium protein fused with GFP has resulted in mice with green fluorescent skin. Thus, GFP is an all-natural biological marker, which is not poisonous, and the properties of which can be controlled accurately [14]. It is therefore important to understand the biophysical basis of its fluorescence, because they open the way of making its analogues with properties required for molecular biology research.

GFP is a water-soluble protein Its three-dimensional structure was determined in 1996 by Ormo and coworkers [17]. The protein globule is a barrel of beta-sheets (Fig. 22A, B) that encapsulates and isolates the autocatalytically formed chromophore (Fig. 22C) from the environment. The chromophore itself consists of a phenole ring, with the OH group protonated inside the protein, and imidazole ring with two nitrogen atoms. The π–conjugated bond system, responsible for the absorption in the visible range, spans both rings. GFP absorbs violet light (around 400 nm), however, the emission is in the green (508 nm). It took some time to understand the reason for such a huge Stokes shift, but the fluorescence upconversion experiments performed by M.Chattoraj et al. finally solved the mystery of green GFP fluorescence [18].

The main result of their investigation is shown in Fig. 23. The researchers recorded upconverted time-resolved fluorescence at 460 nm and 508 nm. Two samples were investigated: one 'normal' GFP, another – dissolved in a buffer, where D_2O was used instead of water. In such conditions, the proton on the phenol ring of GFP is exchanged to deuterium (i.e. becomes two times heavier). From the data, we see that fluorescence at 460 nm appears immediately after the excitation (Fig. 23A,B), which implies that it comes from the same state that absorbs 400 nm photon. In contrast, none of the samples (neither hydrogenated, nor deuterated) shows any 508 nm fluorescence at t=0 (Fig. 23C,D). After about 20 ps in normal GFP and 100 ps in deuterated GFP, initial 460 nm fluorescence decays and the intensity at 508 nm grows in (incidentally, this is the wavelength corresponding to the steady-state fluorescence maximum of GFP). Two important experimental facts here are a) the newly created fluorescence is significantly more intense than the initial signal at 460 nm, and b) *the rate of growth of 508 nm fluorescence depends on whether the phenol ring of GFP chromohore has hydrogen or deuterium attached to it.* These led M.Chattoraj and coworkers to a double conclusion: a) green fluorescence of GFP occurs from a state different from the one that absorbs the photon and b) this state is formed from the initially excited state of GFP via the *proton transfer* (otherwise its

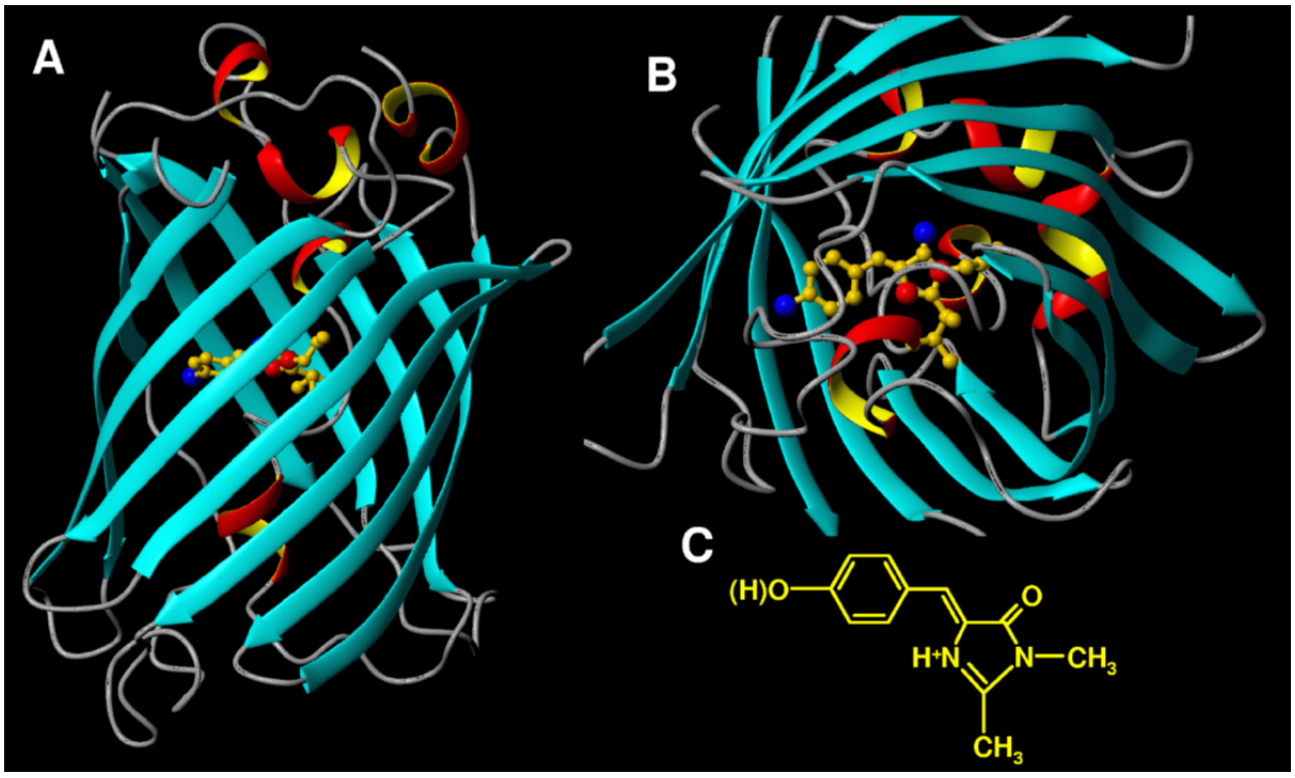

Fig. 22. Three-dimensional structure of GFP viewed from 'the side' (A) and from the 'top' (B). Beta-sheets are shown in green ribbons, and the chromophore is indicated as ball and rod structure. C: Chemical formula of synthetic analogue of GFP chromophore.

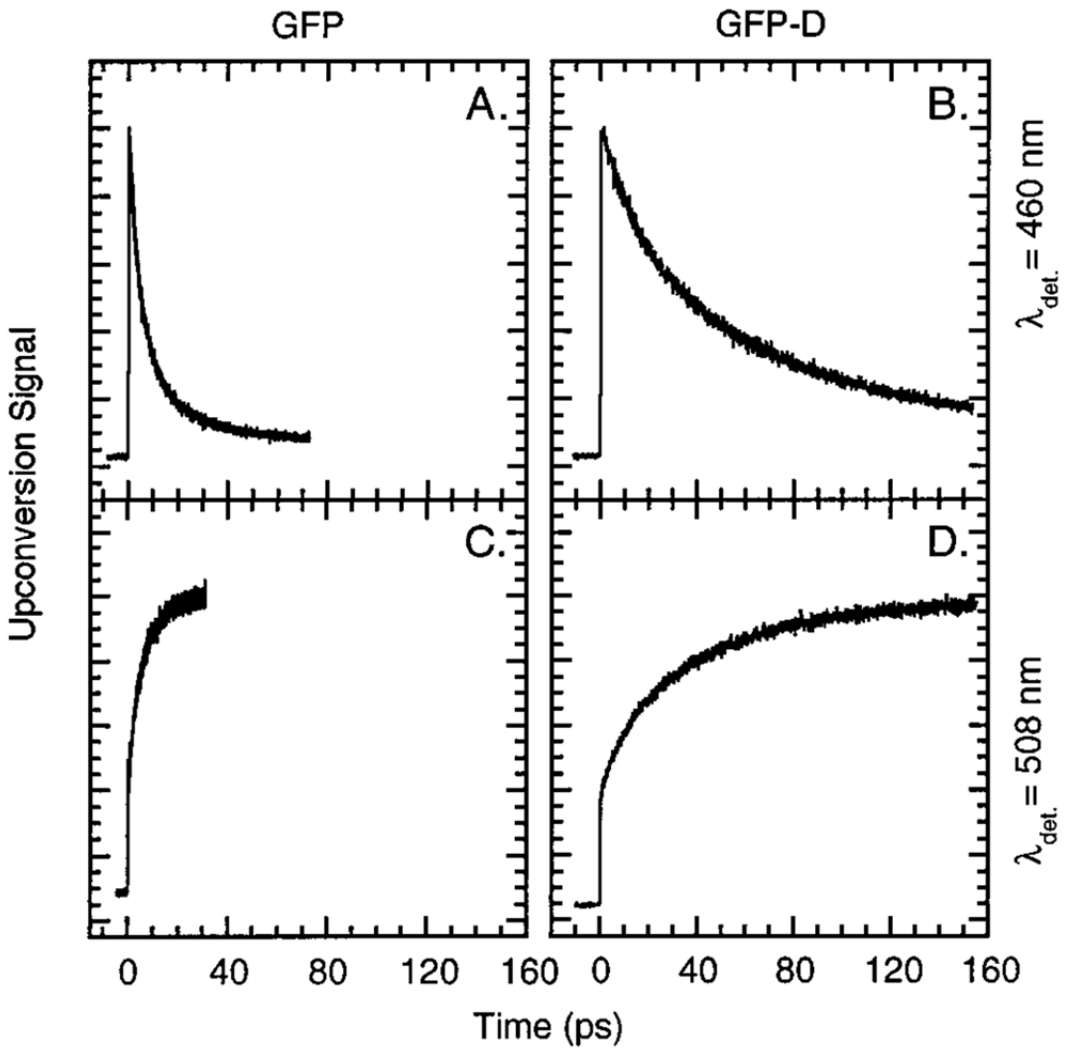

Fig. 23. Fluorescence upconversion experiments in GFP: A, C: fluorescence intensity as a function of time in 'normal' GFP. Panel A shows the kinetics measured at460 nm, whereas panel C shows the fluorescence recorded at 508 nm. B,D – the same experiments as A and C, performed in GFP dissolved in D_2O, where the OH proton of phenol ring is replaced by twice heavier deuterium. Reproduced from [18].

appearance would not be influenced by the effective mass of this proton, i.e. there would be no difference in signals observed in H_2O and D_2O buffers).

This important insight, provided by time-resolved fluorescence experiments, has led to a better understanding of the mechanism of green fluorescence of GFP. In addition, the experimentalists were handed a new interesting toy: a protein molecule, wherein light produces proton transfer. Proton transfer rate observed in this experiment was 8 ps (this is the decay time of 460 nm fluorescence, and the corresponding growth rate of 508 nm fluorescence, see Fig. 23 A, C). These molecules are widely known in chemistry (they are called photoacids), however, this study showed that they are important in biology too.

4.3. Primary photoinduced event in bacteriorhodopsin

Bacteriorhodopsin is a photosynthetic protein of halophilic (salt-liking) bacteria, the function of which is to move the protons across the cell membrane using the energy of light. The detailed functions of this protein are discussed in the context of photosynthesis. Here we will only briefly discuss the aspects of this protein that are necessary for the understanding of the experimental results.

Light absorption in bacteriorhodopsin is performed by retinal – an elongated molecule, similar to carotene, attached to the protein via the Schiff base. The initial photoinduced event finally leading to the proton transfer is the *trans-cis* isomerization of this pigment. The lowest excited state of retinal is of π^* type [19], which is an antibonding orbital, and, contrary to the lowest occupied state, the molecule is free to rotate around a double bond. In order for such rotation to occur, the energy of the excited state has to decrease, as the molecular configuration moves away from planar. At the same

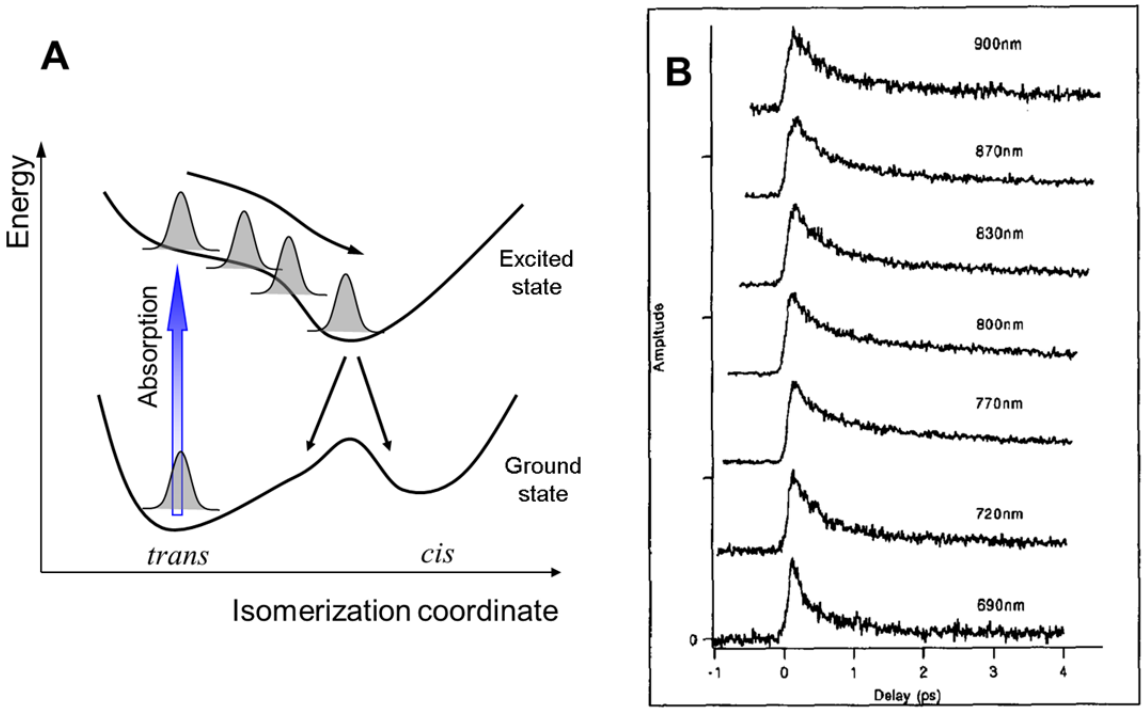

Fig. 24. A: Energy scheme of retinal isomerization (model). The minimum of the excited state corresponds to *cis* molecular conformation. As the molecule moves towards this configuration in the excited state, the energy gap between the states is decreasing, and, at some point, thermally activated vibrational transitions promote the molecule back to ground state. B: Fluorescence decay kinetics at different wavelengths in bacteriorhodopsin. Reproduced from [20].

time, the energy of the ground state is increasing (the ground state has its energy minimum in all-*trans* configuration). Therefore the energy gap between the states is decreasing and, at some point the molecule returns to the ground state (Fig. 24A). If the conformation of the ground state accessible at that point is closer to *cis*, returning to the original *trans* state is impossible because of the energy barrier in the ground state, and retinal ends up being *cis*. The energy accumulated in the deformed chemical bonds of retinal is later used to transport the proton across the cell membrane.

For a long time, experimentalists could not determine the rate of the isomerization process: the time resolution of fluorescence experiments was insufficient and bacteriorodopsin was always faster than the available lasers. All the experiments were forced to conclude merely, that the isomerization rate is comparabale to or faster than time resolution of their experiments. Only in 1993, when first Ti:Sapphire lasers became available, M. Du and G. Fleming could finally measure the decay of excited state of bacteriorhodopsin. The kinetic traces measured in their fluorescence upconversion experiments are shown in Fig. 24B. It is obvious, that the excited state disappears extremely fast: most of the emission decays within the first picosecond. This, then, is the rate, at which bacteriorhodopsin isomerizes inside the protein. Figure 24B also shows that fluorescence is not lost in a single-exponential fashion: some light is still observed after 4 ps (see, for example the kinetic trace in Fig. 24B measured at 800 nm). This indicates that the protein dynamics observed is more complicated than a simple kinetics that can be described by a first-order differential equation. A model is needed to explain such inhomogeneous decay of fluorescence.

It is interesting to note that when retinal is dissolved in an organic solvet, its isomerization becomes a lot slower than inside the bacteriorhodopsin protein [21]. This indicates that evolution has optimized bacteriorhodopsin protein to make the isomerization of retinal as fast as possible in order to use the energy of the absorbed photon most efficiently.

5. Pump-probe spectroscopy: transient absorption measurements

5.1. Experimental technique

In the previous sections we have discussed time-resolved fluorescence measurements, or the intrinsic emission of excited molecules. In this chapter we will discuss another widely used technique of time-resolved spectroscopy, based on the absorption measurement. This is so-called pump-probe (PP) spectroscopy.

An idea of pump-probe measurement is simple: a sample (*e.g.* biologically relevant light absorbing molecule) is excited using a short laser pulse. Another pulse that arrives some time after the first one is used to measure how the absorption of the sample was altered by the first pulse. By varying the arrival time of the second pulse with respect to the first one, we can measure the entire time-dependence of the absorption change. Retroreflector on a motorized translation stage is used to delay one of the pulses, similarly to an autocorrelator (Fig. 11B), or fluorescence upconversion experiment. Thus, for PP experiment, two laser pulses are required: the pump and the probe. Obviously, the pump should be more intense than the probe, because it produces the changes in molecules, whereas the probe merely interrogates them. It would be best, if the probe had completely no influence on the sample being investigated. PP spectroscopy has an advantage compared to time-resolved fluorescence in that the changes of the absorption are sensitive to both the changes in the

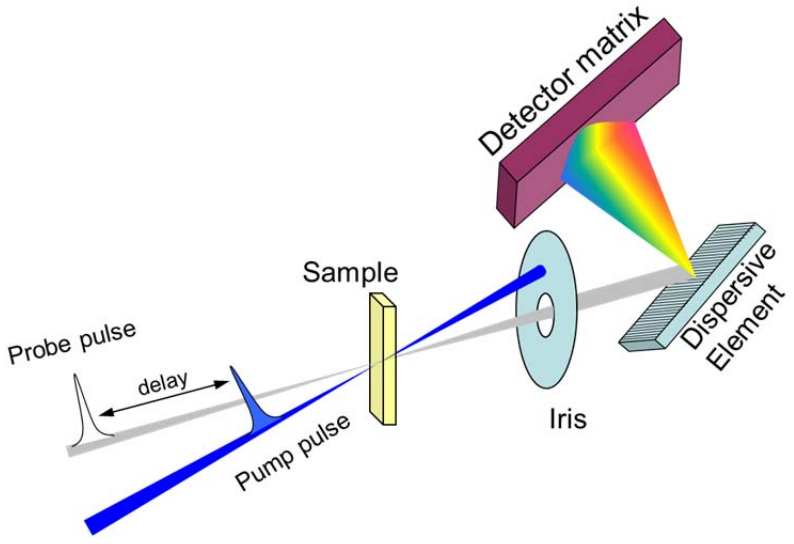

Fig. 25. The idea of pump-probe experiment: pump pulse excites the sample, and probe is used to measure the transmittance. The variable delay between pump and probe pulses provides the time dependence of the difference absorption signal.

ground state and the excited state. Fluorescence always looks at the transitions between the excited and the ground state, and, as soon as the excited state is lost, no signal can be observed any more (even though, the resulting ground state may still be different from the original one, i.e. the effects of the excitation pulse may persist). Free cheese can only be found in mouse traps, and this advantage of PP technique comes with the penalty that the signals contributing to the PP spectra ar more complicated and harder to interpret than those in time-resolved fluorescence. Therefore, both techniques are sometimes combined in order to isolate excited-state information (fluorescence) and obtain a complete ultrafast description of the systems being investigated (pump-probe).

The sample receives two pulses one after the other: the pump and the probe. After passing the sample, the pump is usually blocked, and the probe intensity is measured (Fig. 25). According to the absorption law, probe light intensity behind the excited sample is

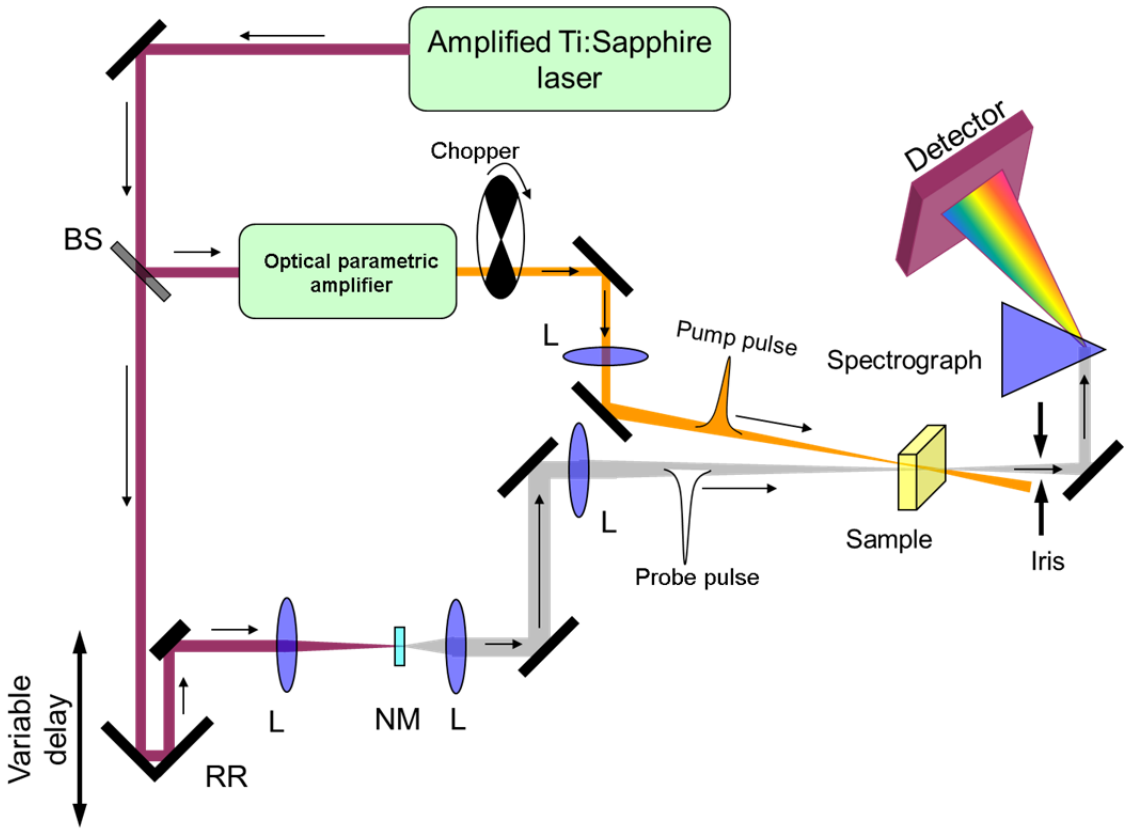

Fig. 26. A: Typical layout of time-resolved difference absorption experiment: amplified pulses from Ti:Sapphire laser are split into two parts using a beamsplitter BS. One part is used to pump an optical parametric amplifer that produces tunable pump pulses. The other part is delayed in a delay line (a retroreflector RR on a motorized translation stage) and then focused into a nonlinear medium NM, where white light supercontinuum is generated (see section 2.1.5). The generated probe light is overlapped with pump light in the sample. The chopper is periodically closing and opening the pump beam in order to take the probe intensity measurements of the excited and non-excited sample).

$$I_{exc} = I_0 \cdot 10^{-A_{exc}} \quad (25).$$

Here I_0 is the intensity of the incident pulse and A_{exc} is the absorption of the excited sample. Analogously, when the pulse is not excited

$$I_{noexc} = I_0 \cdot 10^{-A_{noexc}} \quad (26).$$

By dividing (26) by (25) and taking a logarithm of both sides of the equation, we obtain

$$\Delta A \equiv A_{exc} - A_{noexc} = \lg \frac{I_{noexc}}{I_{exc}} \quad (27).$$

This means that in order to record the absorption change in the sample induced by the excitation pulse, we do not need to measure the intensity of the incident pulse I_0. Absorption change expressed by Eq. (27) is the signal measured in pump-probe spectroscopy. In practice, the layout of the experiment will look something like the one shown in Fig. 25. Ti:Sapphire laser and amplifier produces femtosecond pulses. They are further used in an optical parametric amplifier (or harmonic generator, see section 2.1.5) to obtain the pulses at the wavelengths absorbed by the sample. These become pump pulses. They are periodically blocked and unblocked by an optical chopper (a rotating disc with slots in it) in order to measure both I_{exc} and I_{noexc} in Eq (27). In the visible and near-IR and near-UV spectral range,[6] white light supercontinuum generated in nonlinear medium (sapphire crystal, thin water cell or CaF_2 window) is normally used as a probe. Diffraction grating or prism-based spectral device is used to select desired probe wavelength. The intensity of probe pulses is measured using appropriate detectors (photodiodes or array detectors like CCD, whereby the entire spectrum can be recorded at once). It is important for the detector to be synchronized with the chopper in order to separate the measurements of pumped and unpumped sample. In summary, the spectral dimension of the transient absorption comes from the spectrograph or a monochromator placed behind the sample, whereas the time-resolution is obtained by moving a mechanical delay

[6] When probing in UV, VIS and nIR spectral ranges, we usually interact with electronic molecular excited states, because these wavelengths match the energy gaps between electronic states. If the laser pulses were in the mid-IR spectral range (3-15 μm), we would be doing *vibrational* time-resolved spectroscopy, because the energies of mid-IR photons correspond to the energies of vibrational transitions. In the following, we will stick to electronic time-resolved spectroscopy unless stated otherwise.

line. The measured signal is the function of delay time (period between the pump and the probe pulses) and probe wavelength:

$$\Delta A = \Delta A(t, \lambda) \tag{28}$$

In the further section we will discuss the factors determining the transient absorption spectrum. (28).

5.2. Transient absorption spectrum

We have already stated that PP signals are more complicated than time-resolved fluorescence signals because they contain several different contributions. Let us discuss what these contributions are. For that, let us look at the energy level scheme of a hypothetical molecule shown in Fig. 27A. When the pump pulse excites the sample, some molecules leave the ground state and are transferred to the excited state (solid green arrow). This means that the concentration of ground-state molecules decreases and part of ground state absorption signal disappears. Therefore, at the wavelengths of ground state absorption, the absorption difference (27) becomes negative. The spectral shape of this negative contribution is identical to the ground state absorption spectrum measured by a spectrophotometer (this is what is missing, because some molecules are now in the excited state). This contribution to the difference absorption signal is called *ground state bleaching* (GSB) and is shown in Fig. 27B by green area curve. Over time, this signal remains until all the excited molecules return to the original ground state, from which they were excited.

Another contribution to the PP signal is related with stimulated emission (SE). It arises, when the probe pulse finds some of the molecules in the excited state, and the photons of the probe pulse *stimulate the emission* of the sample molecules (red dashed arrow in Fig. 27A). This the phenomenon underlying the principle of lasers. The photons radiated by the molecules have exactly the same polarization, direction and wavelength as the photons that 'dropped' the molecules from the excited to the ground state. It is easy to see that this signal, similarly to the GSB signal, will be negative: as equation (27) suggests, when the pump pulse is blocked, the number of photons reaching the detector (intensity I_{noexc}), will be equal to the number of photons impinging on the sample (assuming no absorption). When the pump pulse is unblocked, the detector will also receive all these photons *plus the photons emited by the sample*. We will then have $I_{exc} > I_{noexc}$ and signal ΔA in (27) will be negative. It sounds like a paradox: how can you have a decrease in absorption in the spectral range, where sample does not absorb? But it isn't, really. The sample emits light and that is

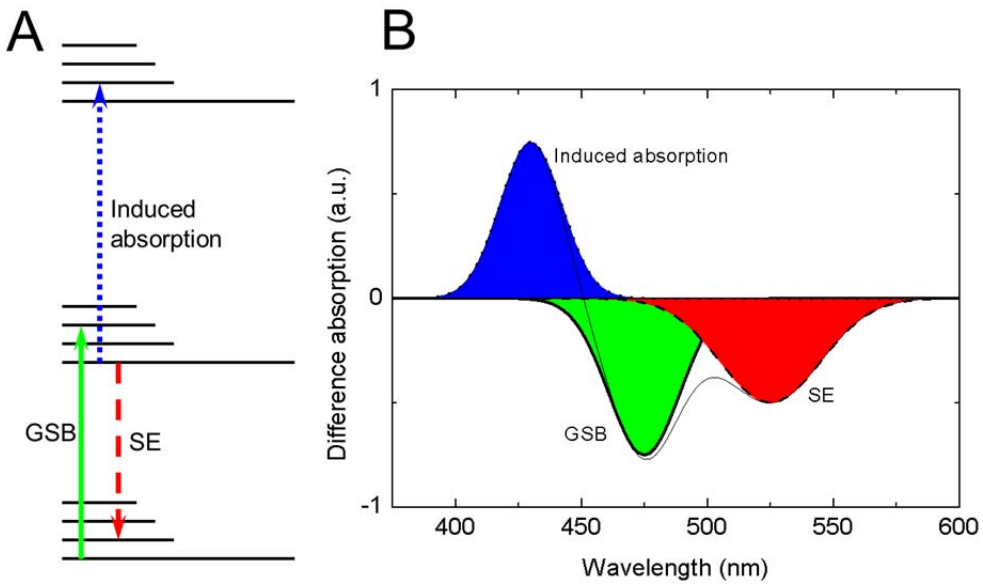

Fig. 27. A. Energy levels of a hypothetical molecule and some quantum transitions influencing the difference absorption spectrum. B: The corresponding difference absorption spectrum and with separated contributions of different transtions.

perceived as decreased absorption. Within the limits of Einstein coefficients, the relationship between the stimulated and spontaneous emission (fluorescence) spectra is:

$$F(\nu) = \frac{8\pi h\nu^3}{c^3} SE(\nu) \qquad (29).$$

In practice this means that in molecular solutions, SE and fluorescence have nearly identical spectral shapes. Similarly to fluorescence, SE exhibits Stokes shift (red shift compared to the absorption spectrum). In Fig. 27B, SE is depicted by the red area curve. The reason for the Stokes shift is the relaxation of the molecule and its immediate environment in the excited state (discussed in detail below).

The third contribution to the PP signal is induced absorption (IA) resulting from the fact that the molecules in the excited state can absorb another photon and go to a higher excited state (dotted blue line in Fig. 27A). This process can only occur in the excited molecules, therefore, after the excitation, *additional absorption* appears and the related contribution to ΔA signal is always positive (blue area curve in Fig. 27B). Note, however, that induced absorption can be caused not just by singlet excited states of molecules. If, for example, the excited molecule has udergone intersystem crossing to the triplet excited state, triplet state absorption will be observed, corresponding to transitions $T_1 \rightarrow T_n$. Even if the molecule is back in the ground state, but this state is slightly different from the initial one (for example, the molecule has isomerized, given away or bound a

proton, the environment of the molecule is hotter than before, and so on), we will observe induced absorption of the new ground state. This is the advantage of PP spectroscopy compared to time-resolved fluorescence: when the excited state is gone, so is the fluorescence signal. Difference absorption remains, though, and can provide information about the further results of photon absorption in the molecule.

5.3. The dynamics of transient absorption spectrum

From the first glance, it seems that the interpretation of spectral and kinetic information of difference absorption spectra is quite simple: all the contributions to the signals (GSB, SE and IA) are proportional to the population of the excited state and all decay in unison. Indeed, in the most primitive cases, this is what we will observe. After the excitation of the molecule, a difference absorption spectrum will appear and uniformly decay with a characteristic time, equal to the lifetime of the excited state, analogously to the Eq. (20). In real life, however, the molecules are more complex than this: they jiggle around, interact with their environment (protein, solvent, solid state matrix, etc.). All sorts of processes may occur after the excitation and they all influence the difference absorption spectrum one way or another.

Let us discuss some of these processes.

1. Internal conversion and vibrational relaxation. The molecules have a number of electronic states, each of which, in turn, has its vibrational sublevels. When the molecule is excited to the higher vibrational sublevels of an electronic state, it seeks to establish the Boltzman distribution (k_BT is roughly 25 meV at 300 K, which is comparable to the typical energy spacing between vibrational sublevels) and the molecule will relax to the lower vibrational sublevels. Since the energy of the excited states is decreasing during such relaxation, the transient absorption spectrum will reflect this relaxation. For example, the wavelength of SE at each time instance depends on the energy gap between the *excited state occupied at that particular instance* and the ground state. Vibrational relaxation can also be observed in the IA signal, because the wavelength of the IA matches the energy gap between the *excited state occupied at that particular instance* and the higher excited state. Therfore, when we put the molecule, say in S_2 electronic state, we will observe the IA corresponding to transitions $S_2 \to S_{n>2}$, and when the molecule relaxes to S_1, this IA signal will disappear and the absorption corresponding to $S_1 \to S_{n>1}$ transitions will appear. Additionally, if the ensemble of molecules (in macroscopic samples we always work with an ensemble) is distributed in

a number of different vibrational states, SE and IS spectra become broader. When vibrational realaxation takes place, all the molecules of the ensemble gather in their lowest vibrational states, and the broadening decrases. The particular realization depeneds on the molecule, but it is safe to say that SE and IA spectra are sensitive to the energy redistribution among the vibrational degrees of freedom in the molecule.

2. Solvation and the relaxation of the environment. Each molecule has a certain charge distribution in the ground state, corresponding to the spatial configuration of its nuclei and electrons. The charges of the environment (solvent, protein, etc.) adjust to the molecular configuration in such a way that the overall energy of the system is at its minimum. After the excitation of the molecule, the configuration of its electrons (hence the charge distribution) is instantly changed. The environment charges 'feel' this and readjust first their electrons, and, subsequently, their nuclei to match the charge distribution of the excited molecule. Besides dielectric relaxation (redistribution of electron orbitals) this may include the shifts of solvent nuclei and reorientation of solvent molecules as dipoles. Dielectric relaxation is near-instantaneous, faster than 10 fs. The rearrangement of environment molecules is called solvation; its rate depends on the mobility of solvent molecules and their dipole moments. Typically, they are in the range of picoseconds and tens of picoseconds.[7] Obviously, the energy of the excited state must decrease when solvation takes place. What happens to the ground state energy? Well, it is easy to answer this if we keep in mind that the environment is now adjusted to the *excited state*. Were we to suddenly place the molecule back in the ground state with its charge distribution, the environment 'would not like it', i.e. the energy of the ground state would be *higher* than that of a relaxed ground state. To summarize, solvation reduces the energy of the excited state and increases that of the ground state (Fig. 28A). The energy gap between these states is directly measured by the stimulated emission spectrum. Therefore, SE maximum will shift towards the red upon solvation (Fig. 28B). Note that GSB spectrum will not be sensitive to solvation; it will stay in place, because it represents the absorption that disappeared upon excitation. This absorption disappears at the time instant of excitation and is recovered when the molecule returns to the lowest energy ground state.

[7] A notable exception to this is water solvation, the major part of which occurs within 50 fs.

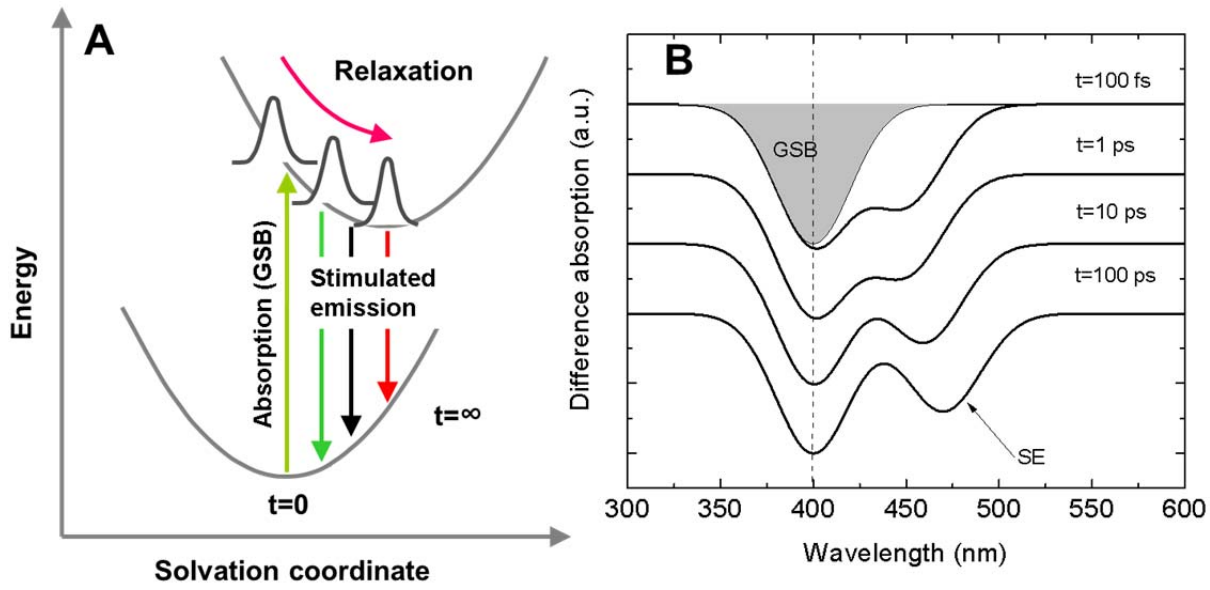

Fig. 28. A. Potential energy surfaces for solvation: when the molecule is excited, the environment reorients to fit the new electronic configuration of the solute. This leads to the decrease of the excited state energy and the increase of ground state energy. As a result, SE spectrum observed in a transient absorption experiment, shifts to the red (B). The GSB spectrum remains unaffected.

3. **Conformational change of the molecule**. Another biologically relevant reaction is the light-induced change in molecular structure. Biological example of this is the photoisomerization of retinal (discussed in section 4.3), from which the photosynthetic process of halophilic bacteria starts. Similar conformational change occurs in rhodopsin – protein residing in the animal retina and responsible for the vision process. There are many types of conformational change and *trans-cis* isomerization is just one of them. Molecules able to undergo conformational changes under light excitation are interesting because of their potential applications in nanotechnology, optoelectronics, information storage, etc. Let us discuss the changes of the transient absorption spectrum resulting from the isomerization of the molecule, similar to the scheme shown in Fig. 24A. Obviously, the ground and excited state energies will follow the same general trend as in the case of solvation (compare the potential energy schemes in Figs. 24A and 28A). This means, one can expect the shift of SE towards the red. After the completion of isomerization and return to a *new* ground state, SE signal will disappear, because there will be no more excited state able to emit photons. However, the ground state will be *different* from the originally excited state. Therefore, we can expect that some GSB will still persist and there will be new IA contribution matching the energy gap between the

new ground state and its excited state. This means that PP spectroscopy allows us to oserve not only the course of photoisomerization, but also the absorption of the product being formed.

4. Formation of a triplet state. Other photoinduced transformations of a molecule, such as triplet state formation, can be analyzed similarly to a conformational change. Triplets hardly emit any light (at least compared to the singlet excited states), therefore, after intersystem crossing, SE signal in transient absorption spectrum will disappear, and the induced absorption of triplet state (corresponding to transitions from T_1 to T_2) will become visible. The GSB signal will persist until the formed triplet state decays.

5. **Excitation energy transfer.** We have already discussed excitation energy transfer. It can be monitored by using both fluorescence and PP spectroscopy. When donor molecule transfers the excitation energy to the acceptor molecule, PP signatures (GSB, SE and IA) will disappear and be replaced by the difference absorption spectrum of excited acceptor. This makes PP spectroscopy and excellent tool to monitor energy transfer between molecules with femtosecond time resolution. Compared to time-resolved fluorescence (where femtosecond resolution is only available in fluorescence upconversion experiments), PP is not just more sensitive (provides better signal-to-noise ratio), but also more flexible, because donor and acceptor populations can be observed at different wavelengths, e.g. at donor excited state absorption and acceptor bleach wavelengths. By selecting the spectral bands appropriately, experiment sensitivity and selectivity can be increased.

6. Proton or electron transfer. Another very important class of photoinduced reactions relates to the photoinduced charge transfer events. Proton transfer occurs in molecules called photoacids and photobases. These are molecules with easily protonating groups (e.g. –OH), the pK_a of which changes upon excitation. Two types of proton transfer are possible: intramolecular, when the proton leaves one group of the molecule and attaches to another group, and proton dissociation, when the proton goes to the environment leaving behind a molecular anion. Electron transfer occurs between electron donor (the molecule that receives excitation) and acceptor, and leads to the formation to two radicals of both molecules. The physical basis of proton transfer is always the same: the excited molecule can reduce its energy by releasing (or capturing) proton or electron. When this charge carrier is caught and stabilized by the molecules in the environment (which could be solvent or acceptor molecules), the donor molecule returns to the ground state, but the charge is not available any more – it is bound to the environment molecules. Therefore, at least for some time, the system remains in the charge-separated state, including radical, ion or isomer. All these reactions are

inevitably accompanied by structural changes in the molecule; often, the molecules acquire a net electric charge. This is necessarily reflected by the change in the absorption spectrum. Following the general logic of analyzing the PP signals, we may expect that initially (at short delay times) we will observe the spectrum of the excited donor (excited states are easy to discern by their SE signals). In a while, this signal will decay and be replaced by new absorption bands, corresponding to the acceptor radical. Note that the GSB of the donor will also remain, because the donor will have become a radical too, rather than returning to its original ground state. In summary, when charge transfer is complete, we can expect to observe: a) donor GSB; b) donor radical (or ion) IA; c) acceptor GSB; d) acceptor radical (or ion) IA. Of course, some of these signals may be weak or lie outside the spectral window of the experiment, in which case they will not be observed.

7. **Photoionization.** Another group of photoinduced events visible in PP experiments are related to photoionization. If the energy of absorbed light quantum is higher than the ionization potential of the molecule, the photon will rip off an electron from the molecule; this electron will be ejected into the environment. This process is instantaneous, and we will not be able to observe the excited state of the molecule. Instead, the excitation will immediately result in the spectrum composed molecular GSB and radical IA. If the molecule is dissolved in liquid or embedded in solid-state matrix, we will also observe the IA spectrum of solvated electron (electron surrounded by oriented solvent molecles). In water, this IA band is very broad (its width is around 0.84 eV) and has a maximum at roughly 720 nm [22]. Note that in ultrafast experiments, when the peak power of excitation pulse is high, photoionization may also be induced by *multi-photon absorption*, the phenomenon when two or more pump photons are absorbed by the molecule at once. In this case, the wavelength of the pump pulse may be longer than the photoionization threshold of the molecule, because the energy of two photons is combined to ionize the molecule. [8]

[8] To answer if the photoionization is one- or two-photon induced, we can measure the pump intensity dependence of radical/electron signals. In the case of single photon ionization, this dependence will be linear, in the case of two-photons - quadratic.

6. Application of transient absorption for the investigation of biological processes: selected examples

6.1. Charge separation in photosynthetic reaction center

Photosynthetic charge separation is one of the most important light-induced reactions in the world. This reaction utilizes the energy coming from the Sun to produce electrochemical potential (proton gradient). The primary charge separation is the electron transfer across the photosynthetic membrane (in the case of bacterial photosynthesis, it is also the cell membrane). This reaction takes place in a specized pigment-protein complex called photosynthetic reaction center. The crystall structure of reaction center found in *Rhodopseudomonas viridis* was determined in 1986 by H.Michel with coworkers [24], and that of *Rhodobacter sphaeroides* was revealed shortly thereafter [25]. Pigment arrangement in the bacterial reaction center is shown in Fig. 29A. Obviously, the reaction center exhibits approximate mirror symmetry. The pigments participating in charge separation are shown in different colors. Two closely spaced bacteriochlorophylls shown in red are called special pair *P*. Slightly 'lower', two 'accesory' bacteriochlorphylls *B* are shown in blue, bacteriopheophytins *H* are in green, and the molecules colored in magenta and cyan are quinons. Electron transfer starts, when the excitation reaches the special pair (the excited state energy of *P* is the lowest among all pigments). The electron first hops onto the accessory bacteriochlorophyll, then onto bacteriopheophytin, and then – onto the first quinon Q_A and the second one Q_B. It is interesting to note that despite apparent symmetry, the electron transfer only occurs via the branch involving the pigments with subscript A (right hand side in Fig. 29A). All the transfer steps, especially the initial ones are ultrafast and only relatively recently – in 1990, W.Zinth with coworkers performed femtosecond pump-probe experiments that revealed the final details of this process [23]. To be able to understand the details of PP experiment, first let us discuss the absorption spectrum of the reaction center shown in Fig. 29B. Different pigments of the reaction center exhibit nicely separated absorption bands (i.e. their excitation energies differ appreciably): the bacteriochlorophylls of the special pair *P* absorb at 870 nm, accessory bacteriochlorophylls *B* have their lowest absorption band at 800 nm, bacteriopheophytins *H* – at 760 nm. These bands correspond to the lowest energy transitions to the states called Q_y. Higher electronic excited states of bacteriochlorophylls called Q_x absorb at 600 nm (Fig. 29B), and those of pheophytins – at 545 nm. It is natural to expect that the bleaching of these bands will occur at the precise instance, when the electron hops onto the pigment

responsible for any particular band. However, we must keep in mind that PP signals also contain other contributions (SE, ESA) and the interpretations of the data have to include all of them.

Transient absorption kinetics of reaction center excited at the special pair *P* absorption band (860 nm pulses were used) are shown in Fig. 30. The curve measured at 920 nm probe wavelength

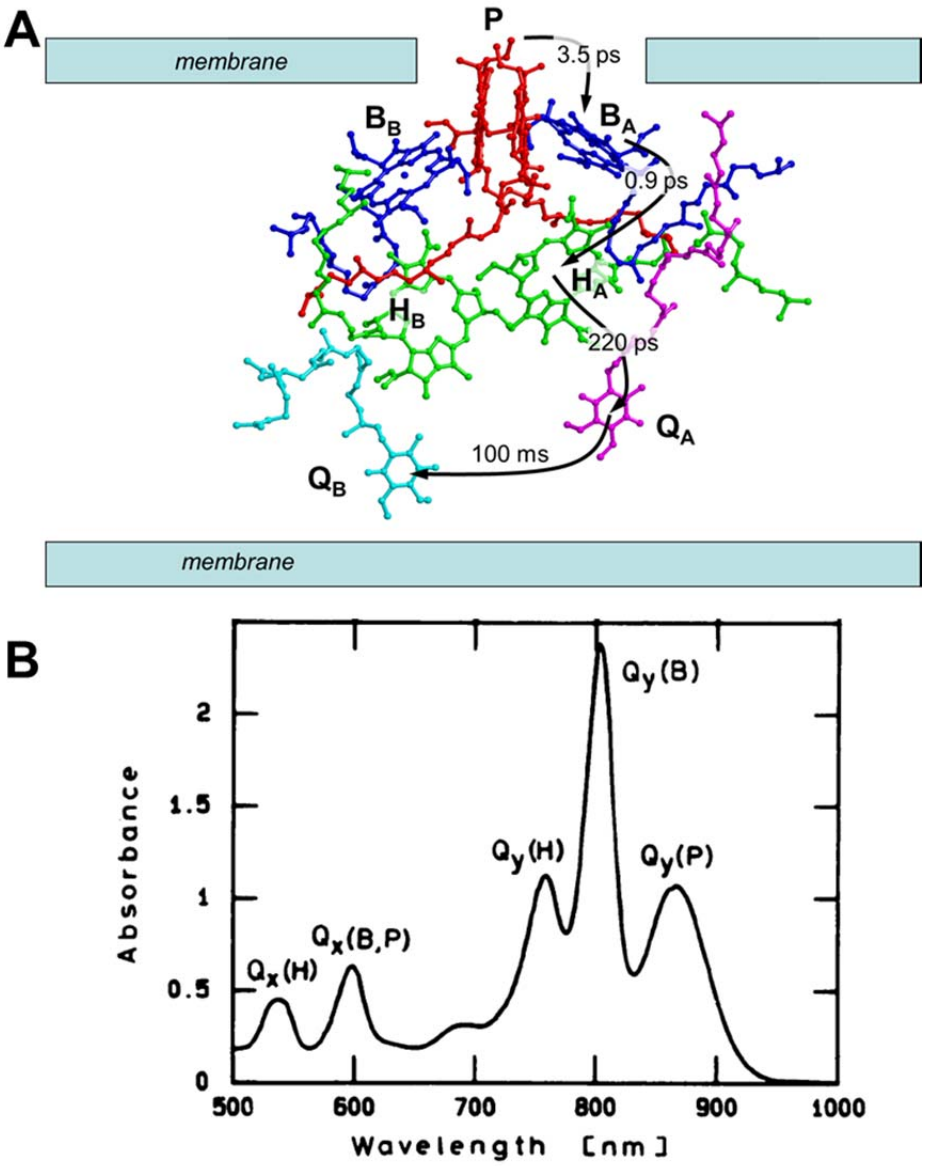

Fig. 29. A. Pigment arrangement in the photosynthetic reaction center of bacterium *Rhodobacter sphaeroides.* Bacteriochlorophylls forming the so-called special pair (*P*) are colored in red, accessory bacteriochlorophylls (*B*) are shown in blue, bacteriopheophytins (*H*) – in green, and quinons (*Q*) – in magenta and cyan. The arrows indicate the pathway of electron transfer and the rates of separate steps. The rates were deterimined from PP spectroscopy by W.Zinth and coworkers [23]. B: Absorption spectrum of *Rhodobacter sphaeroides* [23]. Absorption band of the lowest excited state of the special pair *P* (the transition is denoted Q_y) is at 870 nm, accessory bacteriochlorphylls absorb at 800 nm, bacteriopheophytins *H* – at 760 nm. Higher excited state of bacteriochlorophylls (both *P* and *B*) is denoted Q_x and its absorption band is at 600 nm, whereas bacteriopheophytin absorbs at 545 nm.

(Fig. 30a) is mainly determined by the stimulated emission of the excited special pair *P*. The negative signal appears instantaneously, when *P* is excited and decays in approximately 3.5 ps. This suggests that the excited special pair *P** disappears within this time frame. At later times (when t>10 ps) the signal slightly decays again, which indicates that the dynamics is not over at 3.5 ps. The kinetic trace at 920 nm is well fitted using a three component model (consisting of three decaying exponential functions with lifetimes 3.5 ps, 220 ps and infinity, i.e. a component that persists within the time window of the experiment).

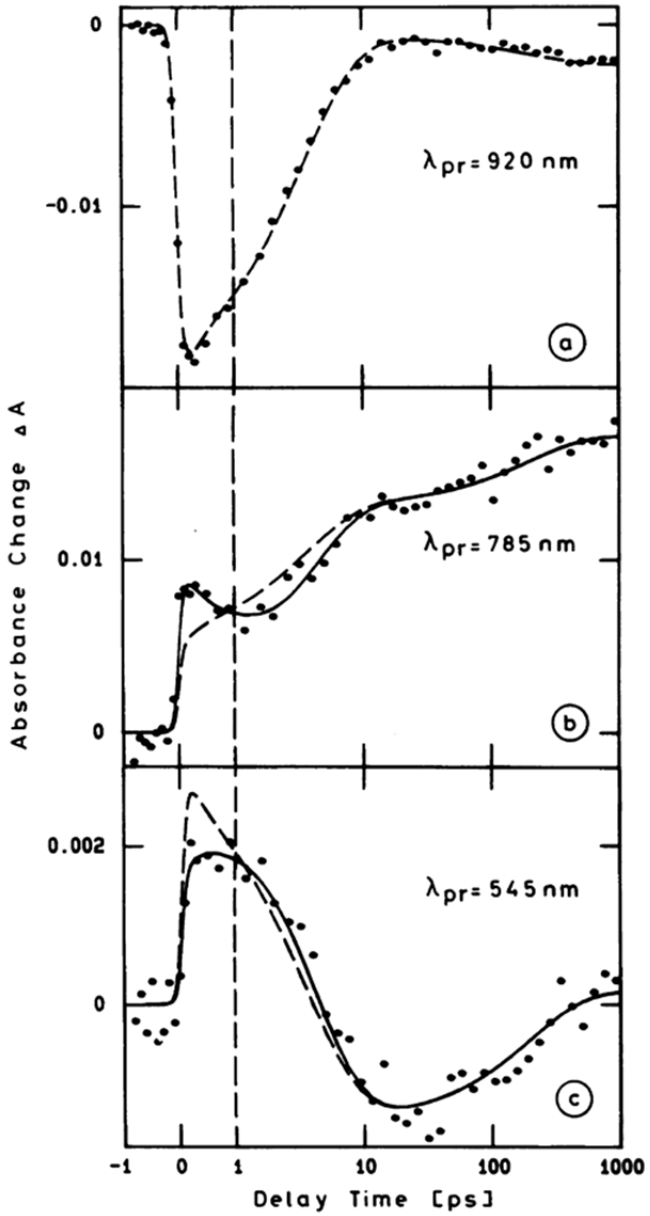

Fig. 30. Transient absorption kinetic traces measured in the reaction center of Rhodobacter sphaeroides, exciting at 860 nm and probing at 920 nm (a), **785 nm (b), and 545 nm (c). The time scale is linear up to 1 ps and logarithmic thereafter. The symbols show experimental data, solid lines – results of modeling obtained using 4 kinetic components, dashed lines – results of 3-component model. Reproduced from [23].**

The absorption change at 785 nm is positive at all times (Fig. 30b). Induced absorption appears immediately after the excitation, decays slightly during the first two picoseconds (the corresponding time constant is approximately 0.9 ps) and starts growing again afterwards. The second phase of signal growth is two-exponential, with time constants of 3.5 ps and 220 ps. The trace at 785 nm cannot be described by just three exponents: if the 0.9 ps component is left out, a clearly unsatisfactory fit is produced, shown in dashed line in Fig. 30b. However, when four-component model is used, the fit is excellent (solid line).

At 545 nm, where bacteriopheophytin *H* has its

absorption peak, complex kinetics is observed: immediately after the excitation, induced absorption is observed, which persists until 2 ps. Later, ΔA starts decreasing and becomes negative (2 ps to 20 ps), and subsequently increases again approaching the zero line (~200 ps times). Again, this kinetic trace cannot be satisfactorily described by three kinetic components, at least four are necessary (compare dashed and solid lines in Fig. 30c). At this wavelength, bacteriopheophytin has its absorption peak, therefore, bleach at this wavelength (negative ΔA) signals about the electron landing on this pigment. The bleaching disappears when the electron moves on to the quinon. Initial positive signal is evidently due to the excited state absorption of P^*, because it appears at the very early times, when the special pair P is excited.

In summary, we have three experimental facts

- P* excited state disappears within 3.5 ps.
- Electron lands on bacteriopheophytin H in ~3.5 ps and moves on within ~220 ps after the excitation.
- Both bacteriopheophytin bleaching and accessory chlorophyll bleaching (785 nm trace) show an additional process with characteristic time of 0.9 ps, i.e. to get an adequate description of the data at least 4 kinetic components are required.

These experimental facts led W.Zinth with coworkers to the following scheme of primary charge separation in the reaction center:

$$P^* \xrightarrow{3.5\,ps} P^+B^- \xrightarrow{0.9\,ps} P^+H^- \xrightarrow{220\,ps} P^+Q_A^- \qquad (30),$$

i.e. the excited special pair P^* transfers the electron to the accessory bacteriochlorophyll B within 3.5 ps, then the electron quickly shifts to bacteriopheophytin H , from which it reaches the primary quinon Q_A in 220 ps. The electron ‘escapes’ from the accessory bacteriochlorophyll much faster (0.9 ps) than it arrives (3.5 ps), therefore the population of P^+B^- state is very small at all times. This is why this state remained undetected for a long time, and the received wisdom was that the accessory bacteriochlorophyll does not participate in the electron transfer chain. The quality of data and sophisticated modeling performed by W. Zinth and coworkers showed for the first time that this pigment is an integral part of charge separation chain. Later, this was confirmed by other experiments [26].

6.2. Excited states of carotenoids: electronic and vibrational relaxation

One of the most commonly encountered pigments in living organisms are carotenoids. These molecules determine yellow and orange color of autumn leaves, provide colors to fruits and vegetables (tomatoes, oranges), fish and even some birds, such a canary. Besides the obvious ability to aesthetically please one's eyes, carotenoids are also important for their biological functions. Perhaps the most important one is the absorption of light used for photosynthesis in plants, bacteria and algae. The main photosynthetic pigments, chlorophylls, do not absorb green and yellow light (this is why they look green). In the meantime, our Sun is a yellow star, and radiates most of its energy in the green-yellow range of the visible spectrum. To make use of all this energy, photosynthetic pigment-protein complexes have evolved to contain carotenoids in addition to chlorophylls. Typical carotenoids absorb in blue-green specral range (420-550 nm) and help chlorophylls in capturing solar energy. In some marine organisms that live in deeper waters, where only blue and green light penetrates, carotenoids are actually the main light absorbing pigments.

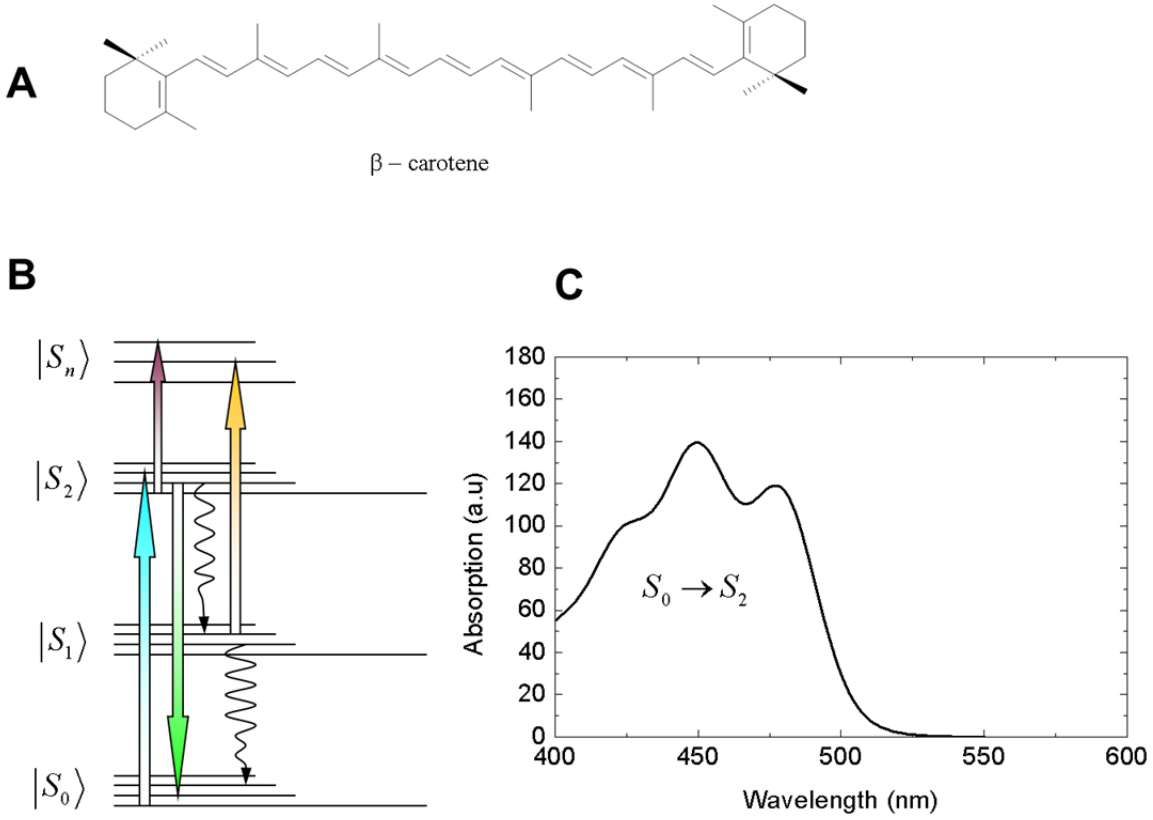

Fig. 31. A: Structural formula of β-carotene, one of the most widespread carotenoids in nature. B: Energy level scheme of a typical carotenoid. C: Absorption spectrum of β-carotene dissolved in hexane. The absorption correspons to the transition from S_0 to S_1 state (blue arrow). Transitions corresponding to $S_2 \rightarrow S_0$ stimulated emission (green arrow), $S_1 \rightarrow S_2$ excited state absorption (orange arrow) and), $S_2 \rightarrow S_N$ excited state absorption (purple arrow) contribute to pump-probe signals. Wiggly lines show radiationless relaxation processes.

All carotenoids have a characteristic polyene structure – a long chain of conjugated double bonds (Fig. 31A). Carotenoids are untypical pigments – they exhibit virtually no fluorescence. This is caused by a peculiar energy level structure: the strong absorption of carotenoids in blue-green spectral range is determined by the transition to the second excited state S_2. The extinction coefficient due to this absorption can be up to 150000 $mol \cdot l^{-1} \cdot cm^{-1}$. In the meantime, the transition from the ground state to the first excited state S_1 is optically forbidden (the symmetry of the S_1 molecular orbital is identical to the one of the ground state S_0, which implies that the matrix element describing the probability of optical transition between S_0 and S_1 is zero).

The structure, energy level scheme and absorption spectrum of a widespread carotenoid, β-carotene (this is the pigment that gives carrots their orange color) is shown in Fig. 31A. When the pigment in the ground state absorbs a photon, it is transferred to the second excited state S_2, which is very short lived and quickly relaxes to the optically forbidden state S_1, which, in turn relaxes to the ground state. All relaxation steps (wiggly lines in Fig. 31B) are radiationless. These processes can be observed and the energy level scheme can be tested by performing PP experiment on β-carotene [27].

The dynamics of transient absorption in β-carotene (solvent: n-hexane) is shown in Fig. 32. The data is plotted as kinetic traces at selected representative probe wavelengths (A) and transient spectra at selected delays. A quick glance at the data reveals that the kinetic traces at different wavelengths are very different, as are the transient spectra. This indicates that an excited β-carotene does not just decay to to the ground state via fluorescence, as a ‘usual’ dye molecule (see Fig. 12 and Eq. (20)). If this were the case, we would observe a monoexponential relaxation with identical kinetic behavior at all probe wavelengths. Instead, the observed pump-probe dynamics is determined by a number of different processes, which are discussed below.

The difference absorption kinetics probed at 420 nm (Fig. 32A, black line) is mainly determined by the ground state bleach (GSB). It is obvious from looking at the transient spectra recorded at different delay times: the region from 400 to 490 nm is all negative and resembles the inverted absorption spectrum shown in Fig. 31C. Both spectra feature a characteristic ‘three-finger’ vibrational structure, and, as expected, the bleaching signal is negative. The kinetic trace at 420 nm shows that the absorption of the ground state decreases immediately after the excitation and the signal goes back to zero within roughly 20 ps. This is the time it takes β-carotene to return to the ground state after the excitation.

At the wavelengths immediately to the red from the red-most absorption maximum, one could expect to observe a negative contribution the difference absorption signal due to stimulated emission (SE). Indeed, the kinetic trace at 495 nm (Fig. 32A, red curve) shows a negative signal immediately after the excitation; however, this signal lasts only 200 fs or less. Later, it is replaced by a small induced absorption (IA). Such fast dynamics at SE wavelength shows that the state into which β-carotene was excited only lives for 200 fs. At the same time, only SE disappears, but the overall signal does not go to zero within 200 fs, neither at this wavelength, nor at GSB. This means that the original ground state population is not yet recovered, but the emitting state population is

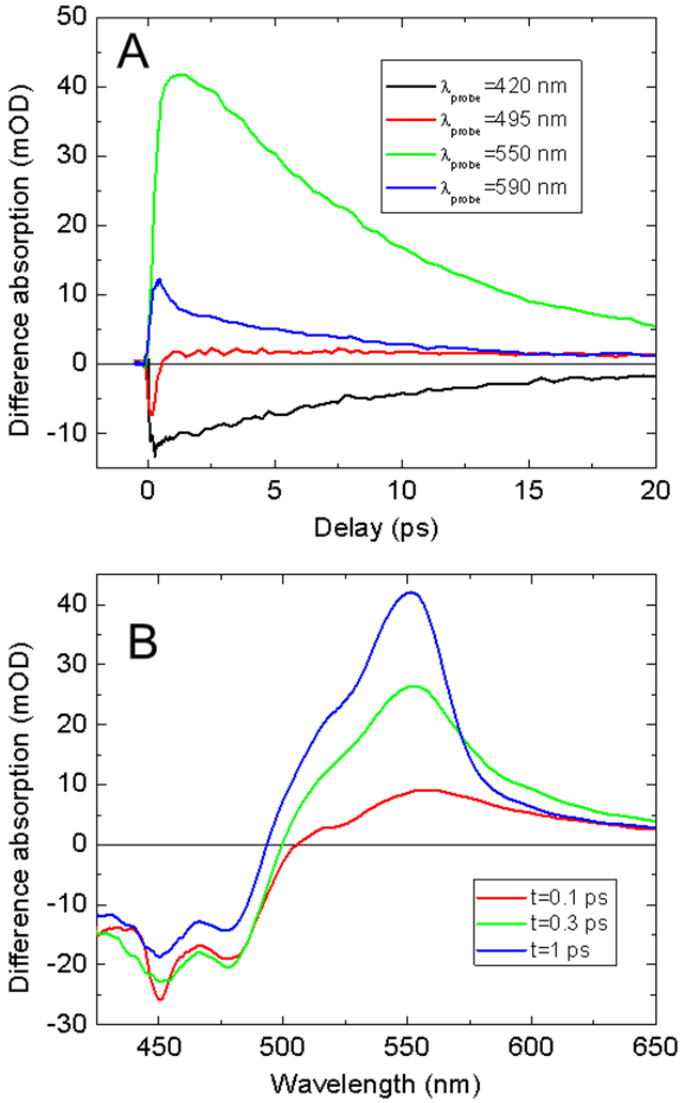

Fig. 32. Difference absorption dynamics in β-carotene dissolved in n-hexane. Panel A shows difference absorption kinetics after exciting the molecules with 400 nm light and probing at 420 nm (black), 495 nm (red), 550 nm (green) and 590 nm (blue). Panel B shows transient absorption spectra at delay times equal to 100 fs (red), 300 fs (green) and 1 ps (blue).

already lost. Transient absorption spectra at delays later than 200 fs exhibit an intense IA band that rises roughly within 200 fs (compare spectra at 100 fs and 300 fs in Fig. 32B). The maximum of this band is at approximately 550 nm. All these experimental facts put together suggest that the S_2 state, into which β-carotene is excited, decays on 200 fs time scale. During this time, the molecule relaxes to S_1 electronic state. The transitions from S_1 to higher electronic states (orange arrow in Fig. 31B) are responsible for the intense excited state absorption (ESA) band centered at 550 nm.

The comparison of transient spectra at 300 fs and 1 ps reveals that the S_1 absorption band becomes narrower and more intense during the time between these two spectra. This is indicative of the vibrational energy redistribution: when the molecule relaxes from the S_2 to S_1, it does it via the ladder of S_1 vibrational sublevels. The population from the higher levels quickly relaxes to the lower ones (within 1 ps). The ensemble of vibrationally excited molecules is distributed over a broader range of energies and therefore has a wider ESA spectrum. Vibrational relaxation is reflected in the kinetic traces at 550 nm and 590 nm (Fig. 32A, green and blue curves). The redder wavelengths mostly represent the ESA of 'hot' S_1 state: signal decays on the time scale of 1 ps, whereas the bluer wavelengths exhibit rise on the same time scale. Within 1 ps, an equilibirium distribution over the vibrational sublevels is reached and IS spectrum remains virtually constant, exhibiting simple decay with the lifetime of S_1 state (~20 ps).

From the analysis above, it is clear that pump-probe experiments allow monitoring a complex excited state dynamics of β-carotene, including, electronic and vibrational relaxation and related spectral changes. Such complex dynamics is observed in all carotenoids, and in some is complicated further by the involvement of not just S_2, 'hot' S_1 and 'cold' S_1 states, but also charge transfer states. [27].

6.3. Energy transfer from carotenoids to bacteriochlorophylls in the photosynthetic light-harvesting complexes

In this section, we once again look into the excited state dynamics of carotenoids. This time, however, we will look at these molecules embedded in photosynthetic pigment-protein complexes, rather than freely floating in solution. The protein in question is the light harvesting antenna complex LH2 of bacterium *Rhodobacter sphaeroides*. Its structure and energy transfer functions were introduced in section 4.1.

After the excitation of carotenoid molecule (LH2 of *Rhodobacter spheroids* contains carotenoid called spheroidene), we may expect energy transfer from S_2 state to bacteriochlorophyll (the latter absorbs at 800 nm, or 850 nm, depending on which ring of bacteriochlorophylls are embedded in). Additionally, carotenoid can relax to S_1 state and *then* transfer energy to bacteriochlorophylls. The energy can go both to B800 and B850 bacteriochlorophylls, both of which have Q_x and Q_y electronic states. This makes the overall energy transfer scheme rather complicated (Fig. 33, [28]).

Pump-probe experiments on LH2 in broad probe spectral range have provided detailed understanding of how carotenoids help bacteria to collect solar light. The first such study, where energy transfer from carotenoids to bacteriochlorophylls was observed, is due to A.P Shreve and coworkers [29]. In the further, we will analyze their results shown in Fig. 34.

In the first experiment, B800 bacteriochlorophylls were excited and their dynamics was probed at the same wavelength, namely 800 nm. The results of this experiment are shown in Fig. 34A. Difference absorption kinetics shows that upon the excitation of B800 bacteriochlorophylls, initially we observe decrease in absorption that lasts for roughly 700 fs (see raw data shown by triangles in Fig. 34A). Within 700 fs, the bleaching is replaced by induced absorption because the excitation energy is transferred to B850 bacteriocholorophylls that feature positive signal at 800 nm.[9] Therefore, we conclude that the excitation energy is transferred from B800 to B850 bacteirochlorophylls within 700 fs. The obtained transfer rate beautifully matches the number yielded by fluorescence upconversion experiment described in section 4.1.

The second experiment was analogous to the pump-probe experiment on β-caroten in solution, described above. Spheroidene was excited using 480 nm light and probed at 498 nm, 510 nm and 540 nm. Similarly to β-carotene, at 498 and 510 nm we observe the S_2 stimulated emission – a negative difference absorption signal at early times. After the decay of this signal, S_1 excited state absorption appears at 540 nm and, to some extent, at 510 nm. Rise of this signal and the start of its decay is discernible in the data. So far, all the observations are analogous to the dynamics observed in solution: LH2 carotenoids are excited into S_2, and subsequently relax to S_1 on 100 fs time scale. The lowest excited states decays within approximately 20 ps (the start of decay is clearly visible in the kinetic trace probed at 540 nm in Fig. 34B).

[9] This signal was observed by exciting B850 bacteriochlorophylls directly.

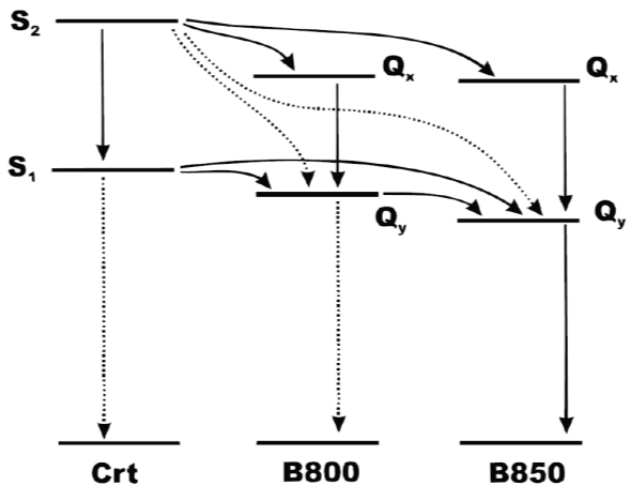

Fig. 33. Generalized scheme of energy transfer pathways in LH2. Reproduced from [28].

The important question, however, is: do S_1 and/or S_2 transfer their energy to bacteriochlophylls, and, if so, how fast is this transfer? This question was answered by another PP experiment, the results of which are shown in Fig. 34C. In this experiment, the spheroidenes were excited using 510 nm pulses and the absorption change was monitored at B800 absorption band. The corresponding difference absorption trace shows that B800 band is bleached almost simultaneously with carotenoid excitation. This means that it has to receive energy from S_2 during the lifetime of this state (which is of the order of 100 fs, as stated above). If the energy were transferred to B800 bacteriochlorophylls *only* from S_2, their bleach should disappear within 700 fs, as is the case when B800 is excited directly (Fig. 34A). The experiment, however, shows a different behavior: B800 bleach after carotenoid excitation persists significantly longer and disappears only after several picoseconds. The only reasonable explanation for this experimental fact is that S_1 state of spheroidene *also* transfers energy to B800 bacteriochlorophylls during its lifetime. As a result, a dynamic equilibirium between B800 and S_1 is established (i.e. for some time B800 is transferring energy to B850, while also receiving it from S_1). Effectively, the lifetime of B800 population becomes longer, compared to direct B800 excitation.

A.P. Shreve with co-authors have also performed the modeling of experimental data according to the connectivity scheme shown in Fig. 34D. The fitting allowed estimating the energy transfer rates and pathways between different pigment pools in LH2 complex. The estimated time constants are shown next to the corresponding arrows in Fig. 34D.

7. Concluding remarks

We have discussed the methods of time-resolved spectroscopy enabling real-time observation of ultrafast processes in biological systems. We started by a short presentation of spectroscopic 'tools', lasers producing femtosecond light pulses of desired parameters, such as peak intensity, wavelength etc. We have then discussed the principles of short pulse characterization and application of ultrashort laser pulses for the research of ultrafast biological processes. It has hopefully become clear that the spectroscopic techniques based on femtosecond time-resolved emission and absorption of excited molecules provide interesting insights into the functions of nanometric scale biological (and other) objects.

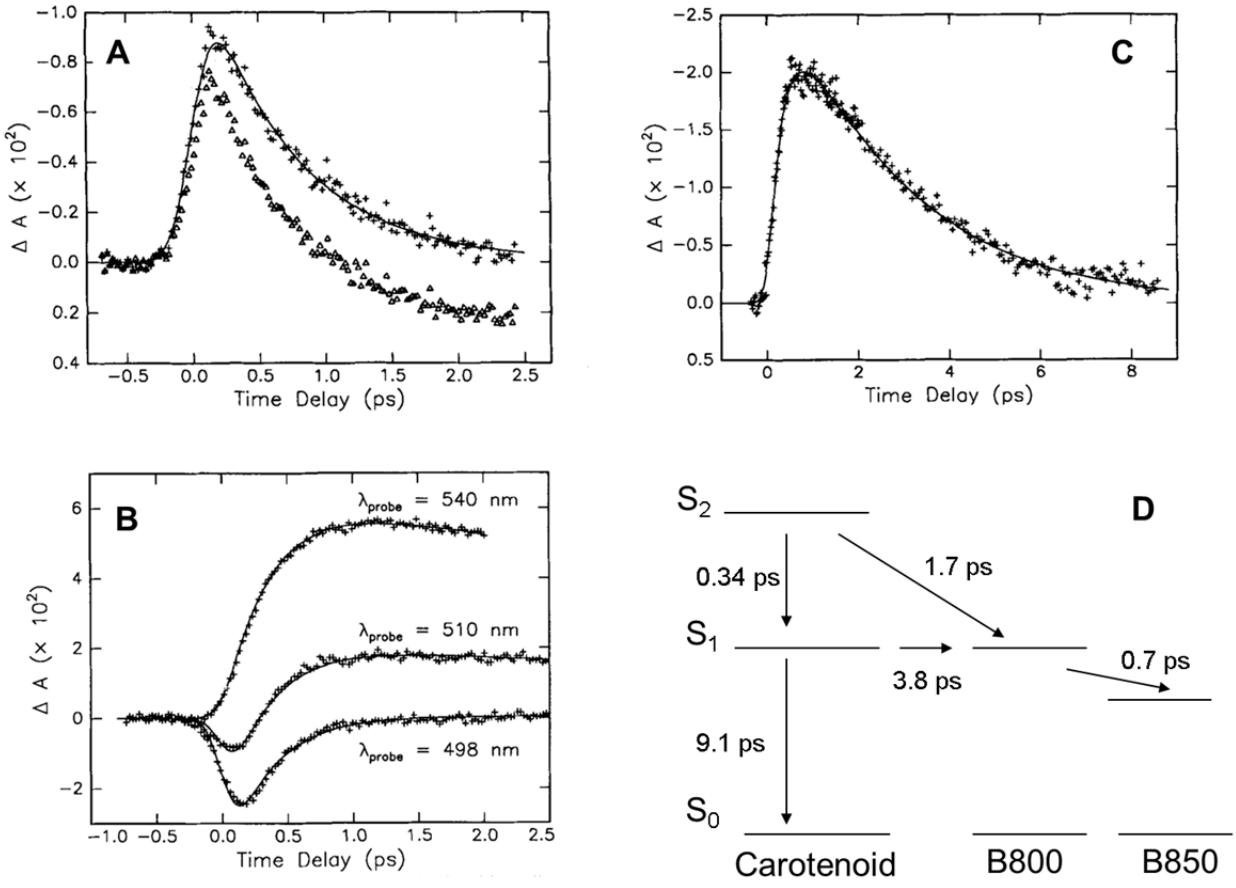

Fig. 34. Pump-probe experiment in the light-harvesting complex LH2 of *Rhodobacter sphaeroides.* A: pump and probe wavelength 800 nm (triangle show experimental data, whereas 'plus' symbols correspond to the data with subtracted B850 excited state absorption, i.e. they show 'pure' GSB of B800); B: excitation wavelength – 480 nm (carotenoid S_2 absorption, see Fig. 19), probe wavelengths are shown on the graph; C: excitation wavelength – 510 nm, probe wavelength 800 nm. The data in this trace are corrected by subtracting B850 ESA signal, i.e. they represent 'pure' B800 bleach. Note the inverted vertical scales in panels A and C. D: the energy transfer times determined from the data. Reproduced from [29].

We have also discussed several examples of applications of ultrafast spectroscopy, and looked into ultrafast biological processes, such as photoinduced proton and electron transfer, excitation energy transfer. The demonstrations have shown how the time-resolved spectroscopic techniques were useful in providing the understanding of such processes.

Finally, we note that such research is not only of academic interest, but also has enormous application potential. The optical computers of the future that may at some point replace current electronic machines require detailed understanding and ability to control picosecond dynamics in nanometric scale logic gates. In the search of alternative energy sources to replace fossil fuels, huge importance is placed on understanding how Nature utilizes solar energy in photosynthesis. To develop artificial photosynthetic systems, it is important to able to test them, establish their parameters, and compare to the natural systems. This is where ultrafast spectroscopy is instrumental.

Generally speaking, the characteristic times of processes taking place in the systems, the dimensions of which are of the order of several nanometers (including all nanoelectronics, nanorobots and other nano-thingies) are bound to be of the orders of picoseconds and femtoseconds. Put simply, the smaller the system, the faster it is ticking. Therefore, the optical time-resolved methods discussed here are one of the main tools opening the doors to the realm of nanometers and femtoseconds.

References

1. Halliday, D., R. Resnick, and J. Walker, *Fundamentals of Physics Extended*. 2007, New York: Wiley. 1328.
2. Rullière, C., *Femtosecond laser pulses: principles and applications*. 2nd ed. 2005, New York: Springer. 426.
3. Koechner, W. and M. Bass, *Solid State Lasers: a Graduate Text*. 2003, New York: Springer-Verlag. 409.
4. Salin, F., *How to manipulate and change the characteristics of laser pulses*, in *Femtosecond laser pulses: principles and applications*, C. Rullière, Editor. 2005, Springer: New York. p. 426.
5. Shen, Y.R., *The Principles of Nonlinear Optics*. 2003, Hoboken, New Jersey: John Wiley & Sons, Inc. 565.
6. Sarger, L. and J. Oberlé, *How to measure characteristics of laser pulses*, in *Femtosecond laser pulses: principles and applications*, C. Rullière, Editor. 2005, Springer: New York. p. 426.
7. Bastiaens, P.I.H. and A. Squire, *Fluorescence lifetime imaging microscopy: spatial resolution of biochemical processes in the cell.* Trends in Cell Biology, 1999. **9**(2): p. 48-52.
8. Jimenez, R. and G.R. Fleming, *Ultrafast Spectroscopy of Photosynthetic Systems*, in *Biophysical Techniques in Photosynthesis*, J. Amesz and A.J. Hoff, Editors. 1996, Kluwer Academic Publishers: Dordrecht. p. 409.
9. Lehninger, A.L., D.L. Nelson, and M.M. Cox, *Lehninger Principles of Biochemistry*. 4th ed. 2004, New York: W H Freeman & Co. 1100.
10. van Amerongen, H., L. Valkunas, and R. van Grondelle, *Photosynthetic Excitons*. 2000, Singapore: World Scientific.
11. McDermott, G., et al., *CRYSTAL-STRUCTURE OF AN INTEGRAL MEMBRANE LIGHT-HARVESTING COMPLEX FROM PHOTOSYNTHETIC BACTERIA.* Nature, 1995. **374**: p. 517-521.
12. Jimenez, R., et al., *Electronic Excitation Transfer in the LH2 Complex of Rhodobacter Sphaeroides.* Journal of Physical Chemistry, 1996. **100**(16): p. 6825-6834.
13. Lakowicz, J.R., *Principles of Fluorescence Spectroscopy. Second Edition*. 2nd ed. 1999, New York: Kluwer Academic. 698.
14. Kendall, J.M. and M.N. Badminton, *Aequorea victoria bioluminescence moves into an exciting new era.* Trends in Biotechnology, 1998. **16**(5): p. 216-224.
15. Chalfie, M., et al., *Green Fluorescent Protein as a Marker for Gene-Expression.* Science, 1994. **263**(5148): p. 802-805.
16. Prasher, D.C., et al., *Primary Structure of the Aequorea-Victoria Green-Fluorescent Protein.* Gene, 1992. **111**(2): p. 229-233.
17. Ormo, M., et al., *Crystal structure of the Aequorea victoria green fluorescent protein.* Science, 1996. **273**(5280): p. 1392-1395.
18. Chattoraj, M., et al., *Ultra-fast excited state dynamics in green fluorescent protein: Multiple states and proton transfer.* Proceedings of the National Academy of Sciences (USA), 1996. **93**: p. 8362-8367.
19. Atkins, P.W., *Physical Chemistry*. 1994, Oxford: Oxford University Press. 1031.

20. Du, M. and G.R. Fleming, *Femtosecond Time-Resolved Fluorescence Spectroscopy of Bacteriorhodopsin - Direct Observation of Excited-State Dynamics in the Primary Step of the Proton Pump Cycle.* Biophysical Chemistry, 1993. **48**(2): p. 101-111.
21. Zgrablic, G., et al., *Ultrafast Excited State Dynamics of the Protonated Schiff Base of All-trans Retinal in Solvents*
10.1529/biophysj.104.046094. Biophys. J., 2005. **88**(4): p. 2779-2788.
22. Boag, J.W. and E.J. Hart, *Absorption Spectra in Irradiated Water and Some Solutions: Absorption Spectra of 'Hydrated' Electron.* Nature, 1963. **197**: p. 45-47.
23. Holzapfel, W., et al., *Initial Electron-Transfer in the Reaction Center from Rhodobacter-Sphaeroides.* Proceedings of the National Academy of Sciences of the United States of America, 1990. **87**(13): p. 5168-5172.
24. Deisenhofer, J., et al., *Structure of the protein subunits in the photosynthetic reaction centre of Rhodopseudomonas viridis at 3[angst] resolution.* 1985. **318**(6047): p. 618-624.
25. Allen, J.P., et al., *Structure of the Reaction Center from Rhodobacter Sphaeroides R-26: The Cofactors*
10.1073/pnas.84.16.5730. PNAS, 1987. **84**(16): p. 5730-5734.
26. Arlt, T., et al., *The Accessory Bacteriochlorophyll: A Real Electron Carrier in Primary Photosynthesis*
10.1073/pnas.90.24.11757. PNAS, 1993. **90**(24): p. 11757-11761.
27. Polivka, T. and V. Sundstrom, *Ultrafast Dynamics of Carotenoid Excited States - From Solution to Natural and Artificial Systems.* Chemical Reviews, 2004. **104**(4): p. 2021-.
28. Sundstrom, V., T. Pullerits, and R. van Grondelle, *Photosynthetic light-harvesting: Reconciling dynamics and structure of purple bacterial LH2 reveals function of photosynthetic unit.* Journal of Physical Chemistry B, 1999. **103**(13): p. 2327-2346.
29. Shreve, A.P., et al., *Femtosecond Energy-Transfer Processes in the B800-850 Light-Harvesting Complex of Rhodobacter-Sphaeroides-2.4.1.* Biochimica Et Biophysica Acta, 1991. **1058**(2): p. 280-288.